# Multi-tool assessment of energy balance consequences of reservoir construction for hydropower generation in the Tropical Andes

Leonardo Antonio Álvarez Guerrero

Tesis de maestría presentada para optar al título de Magíster en Ingeniería Ambiental

Director

Juan Camilo Villegas Palacio, PostDoctor (PostDoc) en Recursos Naturales

Universidad de Antioquia

Facultad de Ingeniería

Maestría en Ingeniería Ambiental

Medellín, Antioquia, Colombia

2022

| Cita | Álvarez Guerrero, 2022 [1] |
|---|---|
| **Referencia**<br>Estilo IEEE (2020) | [1] Álvarez Guerrero, L. A. “Multi-tool assessment of energy balance consequences of reservoir construction for hydropower generation in the Tropical Andes”, Tesis de maestría, Maestría en Ingeniería Ambiental, Universidad de Antioquia, Medellín, Antioquia, Colombia, 2022. |



Maestría en Ingeniería Ambiental, Cohorte Seleccione cohorte posgrado.

Grupo de Investigación en Ecología Aplicada.

Proyecto realizado con apoyo de la fundación Sofía Pérez de Soto

# Multi-tool assessment of energy balance consequences of reservoir construction for hydropower generation in the Tropical Andes

Leonardo Antonio Álvarez Guerrero[a,1], Juan Camilo Villegas Palacio[b,2]

[a]*Grupo GIGA Escuela Ambiental Universidad de Antioquia.*
[b]*Grupo de Investigación en Ecología Aplicada. Escuela Ambiental Universidad de Antioquia. Calle 67 No.~53 - 108 Medellín Antioquia Colombia 1226.*

**Abstract**

In many tropical countries, topographic and climatic conditions favor the installation of hydropower infrastructure, considered cleaner and with fewer environmental impacts than other alternatives for power generation. In recent decades, multiple neotropical watersheds have been targeted for reservoir building. These developments generally result in changes on surface characteristics over large areas, including not only the establishment of new water bodies, but also modifications in land use and vegetation cover in surrounding areas. These changes can potentially lead to atmospheric and ecological changes that may result in unaccounted environmental consequences of this kind of infrastructure. Understanding and assessing these impacts is important in countries like Colombia, where approximately 70% of the nation's electricity comes from hydropower generation, with multiple projects built and put into operation over the last decade. In this work, we use a suite of remote sensing products to characterize changes in surface energy balance in the surroundings of three recently installed (Ituango, Quimbo and Topocoro) and one older (Betania) hydropower projects in the tropical Andes of Colombia. We compare the response of LAI, NDVI, energy budget components and temperature, precipitation, humidity and wind speed before and after the establishment of reservoir lakes using MODIS, CERES, GLDAS and CHRS data. Overall, our results indicate changes in albedo due reservoir filling only in flooded areas, as the result of the change in land cover (replacing land vegetation with a water body), but with no significant effects on temperature and precipitation over non flooded areas. In fact, these changes are not strong enough to significantly modify surface energy budgets in surrounding areas beyond the flooded areas, nor to move beyond other changes in land use. In addition, due to the humid climate in this region, changes in energy budget do not alter precipitation regimes significantly, agreeing with previous studies that indicate that this changes are only significant in arid and semiarid regions. Our results highlight the utility of remotely-sensed products to assess the collective effects of major surface changes such as those produced by large infrastructure projects on local-to-regional energy balances and their associated ecological, hydrological and atmospheric consequences.

## 1. Introduction

Over the last decades, the growth in worldwide demand for electricity has led to a sharp increase in the planning and construction of hydropower plants *[66, 50]*. These projects have been particularly controversial in some countries, as hydropower is considered a renewable energy source while, at the same time, their construction and operation modify large areas of terrain by the obstruction of rivers and inland water accumulation *[69]*, potentially affecting ecosystems (both terrestrial and aquatic) and

*Corresponding author
*Email address:* lantonio.alvarez@udea.edu.co (Leonardo Antonio Álvarez Guerrero)
[1]Acknowledgment to: ISAGEN S.A.S, Fundación Sofía Perez de Soto & Sapiencia
[2]Thesis director

local-to-regional surface-atmosphere coupling. Land use/land cover change is, at the global scale, the second-largest source of climate alteration as it modifies the interactions between the surface and the atmosphere via land surface energy balance, which regulates heat and moisture exchanges, interacting with multiple climatic, hydrological, and biogeochemical processes at different spatial and temporal scales *[17, 12, 4]*.

The construction and establishment of reservoirs produces significant changes in local-to-regional land cover/land use, involving losses of vegetation cover that are replaced by water bodies, modifying the biophysical characteristics of the surface *[24, 13, 61, 51]*. Surface biophysical properties and vegetation activity are key factors in the climate system, due to their contribution to terrestrial climate forcing mechanisms, including radiative balance and evaporative cooling *[17, 7, 52, 30, 58, 4, 1, 2, 8, 9, 5, 35, 63]*. In this sense, land cover/land use changes can influence not only the occurrence of atmospheric variations on daily to seasonal time scales *[6, 29, 23, 36, 15]*but also climate extremes such as drought and heat waves *[44, 39, 55, 41]* and planetary boundary processes *[45]*. In consequence, land cover changes such as those produced by reservoir building could produce land-atmosphere feedback processes, that result in modifications of land-atmosphere energy exchange, affecting meteorological and ecological processes and properties *[24]*.

Previous studies on the influence of hydroelectric projects on local-to-regional climate indicate that in arid and semi-arid climates, the presence of reservoirs is associated with the occurrence of intense precipitation, due to the increase in air humidity over the reservoir area *[13]*. In addition, modeling studies indicate that reservoirs can alter the spatial distribution of precipitation in adjacent areas *[59]*. Further, the presence of reservoirs and associated irrigation capabilities can lead to changes in land cover that result in modified composition, function, and structure of vegetation around the water bodies *[18, 28, 34, 10, 46, 51]*. These ecological changes, in turn, can affect hydrological dynamics (particularly soil water content and evapotranspiration), with potential implications for land surface-atmosphere interactions *[45, 49]*.

Reservoirs can also alter surface-atmosphere exchange processes by changing the net radiation at the surface as a result of the difference in albedo and emissivity between the water and land surfaces, which can change the reflected shortwave and emitted longwave radiation components of the surface radiation budget *[32]*. Not only is the net radiation affected, but also its partitioning into latent, sensible, and ground fluxes can be altered, which in turn results in changes in air temperature, humidity, and surface energy storage and release *[43]*. *Degu et al. [13]*, based on observations and reanalysis data, showed a change in the patterns of specific humidity, convective available potential energy (CAPE), and evaporation over the area of influence of large reservoirs in the United States. However, these changes were climate-dependent, as were significant only in dry areas, while no significant changes in these variables were detected in humid and subtropical regions. From a physical point of view, these results are explained by differences in available humidity of the body of water and the surroundings, for example in humid climates the reservoirs are surrounded by vegetation, which stores and releases water, so that the insertion of an artificial body of water does not generate a marked difference in the flow of humidity to the atmosphere, with evaporation and transpiration rates being very similar in magnitude in these climates. The increase in CAPE can be related to changes in hydrological extremes *[47]*, so reservoirs in dry climates may have an impact on increased storm intensity *[13]*. However, this effect cannot be directly attributed to the reservoir without first describing the interactions between surrounding areas and the local atmosphere *[61]*. The potential impacts of reservoirs on climate are not only relevant for the effects they may have on ecosystems and the populations that depend on them but also on the functioning of these types of projects themselves, as hydropower projects depend on the hydrometeorological behavior of the basins and ecosystems surrounding them. The effect of meteorological and climatic variations on the operation of a reservoir is generally well known. However, no studies on the effect that reservoirs can have on these variations are available, such that unforeseen impacts affecting both the environment and the projects themselves are not easily detected *[61, 24]*.

Due to its water supply and topography, the neotropical region has a high potential for hydropower generation, such that more than 150 dams are planned to be built over the next 20 years in this region *[66]*. Although this situation represents an opportunity for the economic development of the region, the environmental and social impacts of these projects are not adequately estimated, preventing the implementation of adequate environmental impact prevention and mitigation actions *[19]*. The potential effects of dam construction and reservoir installation on the energy balance and its components, and ultimately in hydro-meteorological processes, at multiple scales have not been fully explored in this region *[24, 40, 50, 19]*. Importantly, assessing these effects is required for an integral evaluation of the sustainability of these projects, both in terms of environmental effects *[20]* as well as in time, as potential feedbacks between local climate dynamics and water availability in the supply basins may emerge *[24, 64]*.

Despite current advances, land-atmosphere interactions in these systems are still not fully understood, due to several issues: The lack of temporal and spatial coverage of observations to allow evaluating models *[22]*, the incomplete measurement of variables characterizing the soil-vegetation-atmosphere system *[62]* and the high heterogeneity of surface characteristics, which prevents the generalization of results. In consequence, to date, multivariate and multiscale analysis of soil-atmosphere interactions is incomplete and poorly observed *[27, 48, 45]*.

In this paper, we use different data tools and a modeling process to assess the potential effects of recently installed hydropower generation projects on land surface energy balance and its components. We use the most recent large damming projects: Betania (BET), Ituango (ITU), Quimbo (QUI), and Topocoro (TOP), which cover a range of climatic, topographic, and ecological conditions in the tropical Andes of Colombia. We use a suite of remote sensing products and modeling estimations to characterize changes in surface energy balance, biophysical properties, and meteorological variables before and after the establishment of reservoir lakes.

## 2. Data and Methods

In this work, we analyze the potential biophysical and surface energy budget changes and their potential impacts on precipitation and temperature, due to the land cover change associated with the construction and operation of four large hydropower projects in Colombia. We use the three most recently installed reservoirs and a fourth that has been operating since 1987 in the vicinity of one of the three selected reservoirs. For this, we use multiple variables derived from remote sensing products covering a period between 2000 to 2020 for each of the areas of the reservoir (RA) and their influence areas (IA) defined as a rectangle of $40 \times 40$ km around the reservoir centroids. In addition, we analyze the relationships between these variables and meteorological observations from stations located inside or near each reservoir.

### *2.1. Reservoirs*

The selected reservoirs were: Betania (BET), Quimbo (QUI), Ituango (ITU), and Topocoro (TOP), all of them located in the Colombian Andes. These reservoirs, along with being the most recent projects in the country (except for Betania), represent a variety of ecosystem types, flooded areas, and geometric configurations. In table 2 we present a description of the studied reservoirs and in figure 1 we show the location of the reservoirs.

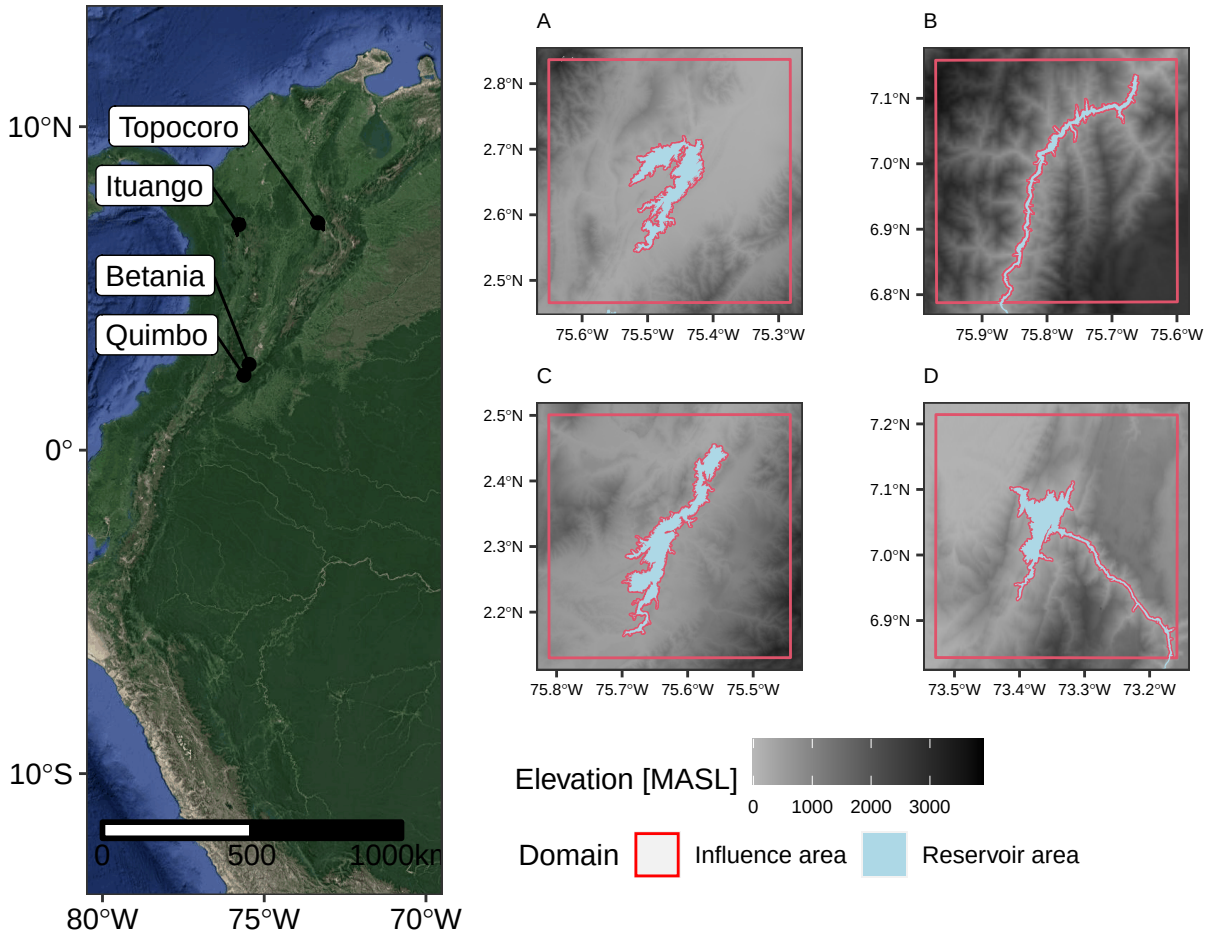


Figure 1: Location of studied reservoirs and sparial domains of study. A. Betania (BET). B. Ituango (ITU). C. Quimbo (QUI). D. Topocoro (TOP)

Also, as a reference to describe the climatic background and ecological setting, we use the Köppen-Geiger classification maps in a resolution of $1 \times 1$ km. *[13, 42]*. Under this scheme, the terrestrial tropics are divided into three main groups – tropical rainforest, tropical monsoon, and tropical wet and dry savanna (grasslands). These groups are all characterized by annual mean temperatures exceeding $18°C$, but are different in their precipitation amount and seasonality. Due to the high elevation in the Andes, under this scheme, some regions were classified as 'Polar', but, given the tropical ecosystem classification for the Andes, we use the name 'Páramo', a characteristic ecosystem of Tropical highlands, to characterize this ecosystem. Also, a similar situation occurs with Temperate climate occurrences, in this case, that will be referred to as "Tropical dry forest". The classification criteria are shown in the table 1.

In table 1 $Pp_{dry}$ is the precipitation of the driest month, $T_{mean}$ is the monthly mean annual temperature, $T_{max}$ maximum monthly temperature in the year or the temperature of the hottest month, $T_{min}$ minimum monthly temperature in the year or temperature of the coldest month and $M_{10°C}$ is the number of months where the temperature is above $10°C$. This variety of environmental settings allowed us to evaluate the potential effects of reservoir establishment in a representative sample of the ecosystems present in the Andes of Colombia. For instance, Topocoro and Quimbo are located in areas that mostly correspond to Tropical rainforests, while Ituango occurs mostly in tropical dry

Table 1: Köppen-Geiger clasification criteria aplicable to studied reservoirs. Adapted from Peel et al., 2007

| **Ecosystem clasification** | **First criteria** | **Second criteria** | **Third criteria** |
|---|---|---|---|
| Tropical rainforest | $T_{mean} > 18°C$ | $P_{dry} \geq 60mm$ | |
| Tropical monsoon | $T_{mean} > 18°C$ | $P_{dry} < 60mm$ | $P_{dry} < 100 - (P_{mean}/25)$ |
| Tropical wet and dry savanna | $T_{mean} > 18°C$ | $Pp_{dry} < 60mm$ | $P_{dry} \geq 100 - (Pp_{mean}/25)$ |
| Tropical dry forest | $10°C < T_{max} < 22°C$ | $0°C < T_{min} < 18°C$ | $M_{10°C} \geq 4$ |
| Páramo | $0°C < T_{max} < 10°C$ | | |

Table 2: Summary of ecosystem types, climatic and physical properties of the studied reservoir areas.

| | **Reservoir** | | | |
|---|---|---|---|---|
| **Variable** | **Betania** | **Ituango** | **Quimbo** | **Topocoro** |
| Tropical rainforest (%) | 21.38 | 39.72 | 70.19 | 84.99 |
| Tropical Monsoon (%) | 60.33 | 15.03 | 17.81 | 7.51 |
| Tropical Grassland (%) | 14.57 | 0.15 | 0.21 | 3.59 |
| Tropical dry forest (%) | 3.72 | 43.85 | 11.58 | 3.91 |
| Páramo (%) | 0 | 1.24 | 0.21 | 0 |
| Shore development | 14.84 | 18.47 | 17.34 | 12.82 |
| Reservoir Area ($hm^2$) | 6881.00 | 3810.30 | 8318.20 | 6989.30 |
| Latitude ($°N$) | 2.65 | 6.97 | 2.31 | 7.03 |
| Longitude ($°E$) | -75.47 | -75.78 | -75.63 | -73.34 |
| Altitude ($m.a.s.l$) | 659.00 | 695.00 | 840.00 | 555.00 |

forests and Betania (the oldest) in the tropical monsoon ecosystem. While Ituango is lesser extent reservoir, also has the longest shoreline, indicating a more elongated shape than, for instance, Topocoro or Betania, with larger areas and lower shore development values. In addition, these reservoirs cover a gradient of altitude that relates to multiple environmental factors such as meteorological and ecological features.

### *2.2. Data sources*

#### *2.2.1. Biophysical characterization:*

To describe biophysical changes we use $LAI$ and $NDVI$ measurements from MODIS for each reservoir and area of influence, which allow us to detect the timing of land cover/land use change and possible alterations in vegetation after the flooding process of the reservoirs.

#### *2.2.2. Surface energy and radiation balance*

To describe the changes in land surface energy balance due to reservoir building, we analyze their different components using remote sensing products (table 3) in each one of the studied Reservoirs Areas (RA) and in a rectangular area of $40 \times 40$ $km^2$ around each one of them named Influence Area (IA). Also, we analyze radiation and energy balance components obtained from the CERES EBAF product which allows us to characterize incoming and outgoing radiation in shortwave and longwave components and cloud conditions for 1° grids. The data comprises the period between 2002 and 2020, with different spatial and temporal resolutions due to differences in the retrieving methods for each variable inside the MODIS mission. The analyzed variables were: Land surface temperature in day and night conditions, land surface emissivity (bands 29,31,32), evapotranspiration, latent heat flux, and albedo. To describe the land surface changes associated with the reservoirs we use Colombia's environmental authority open access information about reservoirs delimitation. MODIS data were processed using the different product quality assessment bands and removing low-quality values. After this, we create a time series of each variable for reservoir areas and adjacent land areas. We use the

Table 3: Summary of MODIS remote sensing products used

| Product | Description | Frequency | Resolution (m) |
|---|---|---|---|
| MCD15A2H | Terra+Aqua Leaf Area Index/FPAR | 8 day | 500 |
| MCD19A3 | Terra+Aqua BRDF Model Parameters | 8 day | 1000 |
| MCD43A | Terra+Aqua BRDF and Calculated Albedo | 1 day | 500 |
| MCD43A1 | Terra+Aqua BRDF/Albedo Model Parameters | 1 day | 500 |
| MOD11A2 | Terra Land Surface Temperature and Emissivity | 8 day | 1000 |
| MOD16A2 | Terra Net Evapotranspiration | 8 day | 500 |
| MOD21A2 | Terra Land Surface Temperature/3-Band Emissivity | 8 day | 1000 |
| MYD16A2 | Aqua Net Evapotranspiration | 8 day | 500 |
| MYD21A2 | Aqua Land Surface Temperature/3-Band Emissivity | 8 day | 1000 |

CERES data *[33]* from 2002 to 2020, specifically the variables of incoming shortwave and longwave radiation, for all cloud conditions and cloud areas, each one of these variables in monthly frequency.

To evaluate changes in other meteorological variables, we use data from the Global Land Data Assimilation System (GLDAS), corresponding to wind speed, specific humidity, and precipitation over the studied areas from 2000 to 2021. Also, to obtain a gridded reference in precipitation changes, we use the PERSIANN-Cloud Classification System (PERSIANN-CCS), which is a global high resolution ($4 \times 4$ $km$) satellite precipitation product developed by the Center for Hydrometeorology and Remote Sensing (CHRS). Considering the influence in the region of climate variability phenomena, we analyze the potential association of meteorological changes with the occurrence of El Niño-Southern Oscillation (ENSO) using the ONI index for each month in the studied period from the NOAA Climate Prediction Center.

### *2.3. Data processing and stadistical analysis*

#### *2.3.1. Reservoir biophysical characterization*

We characterize the selected reservoirs using morphometric measurements including reservoir surface area ($A$) and shore development ($D_l$) *[57]*; that is the ratio of the length of the shoreline to the length of the circumference of a circle of area equal to that of the lake:

$$D_l = \frac{L}{2\sqrt{A}} \tag{1}$$

The closer this ratio is to 1, the more circular the lake, while, larger ratios ($D_l \gg 1$) indicate the shoreline is more complex and possess a higher potential for the development of vegetal littoral communities and biological productivity.

#### *2.3.2. Surface energy and radiation balance*

To estimate each of the land surface energy balance components, we use a similar approach to *Duveiller et al. [17]*. In this approach air temperature $T$ is calculated as the mean between Day-time and night-time land surface temperature (LST), considering that the MODIS instrument measures twice over its cycle at $\approx$ 13:30 and 1:30 local time at the Equator. The surface upwelling longwave radiation ($LW_{uw}$) is the outgoing infrared radiation emitted by the surface, it can be calculated from temperature ($T$) and broadband emissivity $B$ using the Stefan-Boltzmann law:

$$LW_{uw} = \epsilon_B \sigma T^4 \tag{2}$$

Where is the Stefan-Boltzmann's constant ($5.67 \times 10^{-8}$ $Wm^{-2}K^{-4}$). The Broadband emissivity was calculated from narrowband emissivity in the middle and thermal infrared spectrum measurements by MODIS, following the empirical relationship developed by *Wang [54]*:

$$\epsilon_B = 0.2122\epsilon_{29} + 0.3859\epsilon_{31} + 0.4029\epsilon_{32} \tag{3}$$

Where $\epsilon_{29}$, $\epsilon_{31}$ and $\epsilon_{32}$ are the estimated emissivities in MODIS bands 29 ($8400 - 8700\ nm$), 31 ($10780 - 11280\ nm$) and 32 ($11770 - 12270\ nm$). Satellites can only measure during cloud-free observations, in consecuence the resulting monthly upwelling longwave radiation only refers to clear sky conditions $LW_{uw}^{clear}$. To estimate the efect of cloudiness we used a correction factor based on the proportion of all sky ($LW_{uw_c}^{all}$) to clear sky ($LW_{uw_c}^{clear}$) longwave upwelling radiation estimated by CERES so the longwave emission is estimated as:

$$LW_{uw} = (\frac{LW_{uw_c}^{all}}{LW_{uw_c}^{clear}}) \times LW_{uw}^{clear} \tag{4}$$

We obtained the albedo ($\alpha$) values from the MODIS MCD43C3 product that collects multispectral cloud-free albedo observations over a 16-day moving window and a semi-empirical kernel-driven bidirectional reflectance model. This product brings $8 - day$ estimates of directional hemispherical albedo, known as black-sky albedo ($\alpha_{bs}$), which corresponds to a theoretical value of albedo if incoming radiation is completely direct and bi-hemispherical albedo, known as white-sky albedo ($\alpha_{ws}$) which correspond to a theoretical value of albedo if incoming radiation its completely diffuse. To obtain an estimate of actual albedo we use the following expression *[56]*:

$$\alpha = f_d(\theta_i)\alpha_{ws} + (1 - f_d(\theta_i))\alpha_{bs}(\theta_i) \tag{5}$$

Where $f_d$ is the proportion of diffuse irradiation at a specific solar zenith angle $\theta_i$; the $f_d$ derived from aerosol optical depth (AOD) acquired from the MODIS aerosol product (MOD08). We use these values to estimate the shortwave outgoing radiation changes, multiplying the CERES shortwave incoming radiation values by the albedo values obtained for each studied area.

For latent heat flux estimations we use the MOD16A2 product, which provides latent heat obtained by integrating several MODIS products with meteorological data at 0.05° spatial resolution (corresponding to terrestrial land transpiration). This product corresponds to the daily mean latent heat in 8-day composites ($jm^{-2}day^{-1}$). We convert this variable in to $Wm^{-2}day^{-1}$ dividing by number of seconds in each day (86400 $s$). Because these variables are not fully observation-driven certain values can be outside of a logical range, so we limit the maximum values of latent heat using the net radiation values obtained from the radiation data products and estimations. Furthermore, the latent heat flux estimated is subtracted from the net radiation to obtain the sum of sensible heat fluxes and ground heat fluxes ($H + G$). These allow us to calculate land surface energy balance considering the following expressions:

$$Rn = SW_{dw} - SW_{uw} + LW_{dw} - LW_{uw} = H + \lambda E + G \tag{6}$$

$$H + G = SW_{dw} - \alpha SW_{dw} + LW_{dw} - \epsilon_B \sigma T^4 - \lambda E \tag{7}$$

With these variables, we constructed monthly time series for each one of the components and further we analyzed the decomposed properties of each series for the reservoir area and their surroundings in search of changes in overall trends (for the entire period), seasonal and remaining (or anomalies) components using the developments of *Verbesselt et al. [53]*.

Considering that the remote sensing products do not provide a direct measurement of evaporation in the reservoirs, we used an estimation based on Penman Equation, as shown:

$$\lambda E = \frac{\frac{\Delta}{\gamma} Rn - Ea}{\frac{\Delta}{\gamma} + 1} \tag{8}$$

Where $\Delta$ is the gradient of the slope of the saturated vapor pressure-temperature curve at mean air temperature ($Pa°C^{-1}$), $\gamma$ psychometric constant (depends on temperature and atmospheric pressure;

$Pa°C^{-1}$), $Ea$ corresponds to the evaporation rate in the reservoir which depends on the wind function, that its the effect of wind in humidity production over the reservoir water body and the saturation vapor pressure gradient as shown:

$$Ea = f(U_2)(e_s - e_a) \tag{9}$$

In this work, we use as wind function de developments of *McJannet et al. [38]*, which allows us to estimate the reservoir wind function as an area (A) or fetch (L) (directly associated with RA) and $U_2$ wind speed at 2 m above the reservoir water surface ($ms^{-1}$) dependent function:

$$f(U_2) = (2.36 + 1.67U_2)A^{-0.05} = (2.33 + 1.65U_2)L^{-0.1} \tag{10}$$

*2.3.3. Biophysical properties: LAI and NDVI*

To account for the potential changes in biophysical properties due to reservoir building and operation, we decompose the time series of biophysical variables using a change detection approach by detecting and characterizing Breaks For Additive Seasonal and Trend (BFAST) *[53]*. BFAST is an unsupervised time series change detection algorithm specialised in detecting multiple breakpoints within a multi-year time series. It works by first decomposing an input time series $Y_t$ into trend ($T_t$), seasonal ($S_t$) and error ($e_t$) components using Seasonal decomposition of Time series by Loess (STL) as shown *[11]*:

$$Y_t = T_t + S_t + e_t \tag{11}$$

Next, the trend and season components are tested for at least one significant break in the whole time series using an ordinary least squares residual moving sum (OLS-MOSUM) statistical test. If there is significant evidence ($P < .05$) of a break in either the trend or season component, then a process of fitting a univariate piecewise linear regression to determine the locations of the breakpoints (as defined by *Bai and Perron [3]*) is carried out for each of the components. The decomposition and fitting process is repeated iteratively until convergence is reached *[16]*.

*2.3.4. Spatio-temporal change of biophysical properties*

To identify the regions of changes in the monthly biophysical variables we use a Mann-Kendall test to each one of the pixels in the raster products, which allow us to detect the magnitude of trend variations and their significance in an spatial context.

*2.3.5. Energy balance and climatic variables*

To synthesize the overall changes in meteorological and climatic variables between BL an BL phases for both the IA and RA, we used box-and-whisker plots for each of these four conditions and explored significant differences with a Kruskall-Wallis test. We explore how the different components of land surface energy balance and biophysical properties influence meteorological variables. More specifically, we relate monthly energy balance components with precipitation ($Pp$), day-time surface temperature ($T_d$), night-time surface temperature ($T_n$), wind speed ($W_s$) and specific humidity ($SH$) using Partial Least Squares ($PLS$) regression models, as most of the predictor and outcome variables correlate and can interact with each other. As predictors we use the monthly values of ONI, albedo, shortwave and longwave incoming radiation, longwave emitted radiation, latent heat and the remaining fluxes (sensible and ground fluxes), cloud properties (area, temperature, pressure and optical depth). We used data between 2005 and 2020, corresponding to the co-ocurring period for all these variables. We trained each of the PLS models selecting randomly an 80% of data and tested model performance against the remaining 20%. We also used the BFAST technique to evaluate changes in the temporal development of these relationships.

## 3. Results

### *3.1. Biophysical characterization*

#### *3.1.1. Temporal evolution of LAI in the reservoirs and their Area of influence:*

In figure 2 we show the remainder and trend components of the LAI and NDVI for each one of the reservoirs. LAI values did not exhibit significant changes in their seasonal components, indicating that there is no alteration in vegetation intra-annual variability due reservoir building. However, with the exception of TOP, trends in LAI values did changed, particularly in the RAs (reservoir areas) and their closest vegetation ($< 500\ m$ from reservoir border due LAI product resolution), without a generalizable impact in biophysical characteristics of IAs.

In the TOP reservoir's IA, LAI trend components changed from $3.04 \pm 0.01$ to $3.08 \pm 0.01\ m^2/m^2$ in January 2012. In contrast, RA LAI trend change occurred in October 2014, varying from $3.11 \pm 0.02$ to $1.39 \pm 0.02\ m^2/m^2$, which coincides with the start of this reservoir construction. In the QUI reservoir, which also started construction in 2015, LAI trend changed in April 2015, from $1.98 \pm 0.01$ to $0.94 \pm 0.01\ m^2/m^2$. For ITU reservoir, LAI trend changes in two moments: February 2009 and October 2015. Previously to those changes in trend in the mean, LAI for reservoir area was $2.46 \pm 0.01$ $m^2/m^2$, between the detected changes was $2.47 \pm 0\ m^2/m^2$ and after the final change was $2.02 \pm 0.1$ $m^2/m^2$ which steadily declines until it reaches $1.38\ m^2/m^2$ in December 2020. From the two detected changes, the latter is directly associated with the reservoir building and operation, considering that ITU RA is located in a narrow mountain valley and can be associated with variations in vegetation density due river flow and precipitation increments that can produce eventual landslides and vegetation loss. For BET, RA close vegetation exhibits a rise in the trend in March 2016 ($3.05 \pm 0\ m^2/m^2$ to $3.15 \pm 0\ m^2/m^2$). This change can be attributable to an indirect impact of the reservoir, for example, by fostering vegetation development due to increased water availability. However, this potential effect is constrained to the closest vegetation, considering that IA doesn't show this behavior.

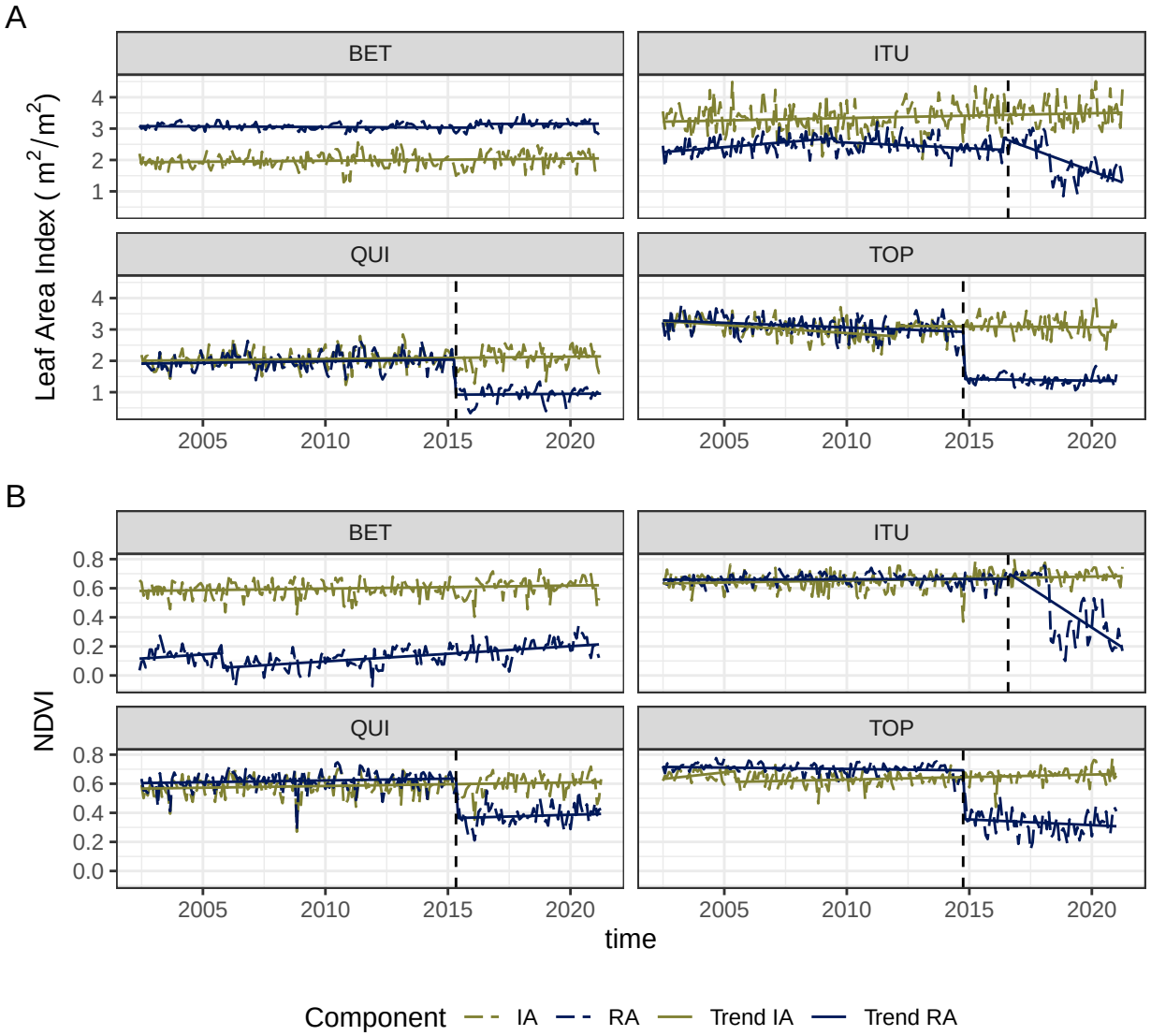


Figure 2: Vegetation index changes in each reservoir and sorrouding areas. A. LAI series. B. NDVI series

*3.1.2. Temporal evolution of NDVI in the reservoirs and their Area of influence:*

Similar to the LAI results, NDVI seasonal components don't systematically change for any one of the studied reservoirs nor their influence areas. Only TOP IA exhibits a change in NDVI trend in June 2005, when it changes from 0.69 to 0.61. However, this change doesn't represent a significant change for the trend component mean value for the periods before and after the change ($NDVI_t = 0.64, P < .05$).

As expected, NDVI trends change in all the RAs, these were: October 2014 in TOP ($0.71 \pm 0.01$ to $0.33 \pm 0.01$); May 2015 in QUI ($0.62 \pm 0.01$ to $0.38 \pm 0.01$); August 2016 in ITU ($0.66 \pm 0.13$ to $0.43 \pm 0.13$); October 2005 in BET ($3.07 \pm 0$ to $3.08 \pm 0$). These changes, with the exception of BET, are coinciding with the starting of the Building & operation phase of the hydroelectric projects.

When contrasting the BL and BO phases of the projects (this comparison represents the conditions

before and after the reservoir, respectively), we find that there is no significant impact of the reservoir building on the dynamics of vegetation density and activity outside the RAs. This can be observed in both the spatial-temporal trends observed using all data (figure 3), where the changes in LAI and NDVI are predominantly limited to the flooded areas, while in the surrounding areas, the general responses are associated with positive and significant trends in LAI but with low magnitude, and less frequent areas with LAI reductions in the case of ITU and TOP.

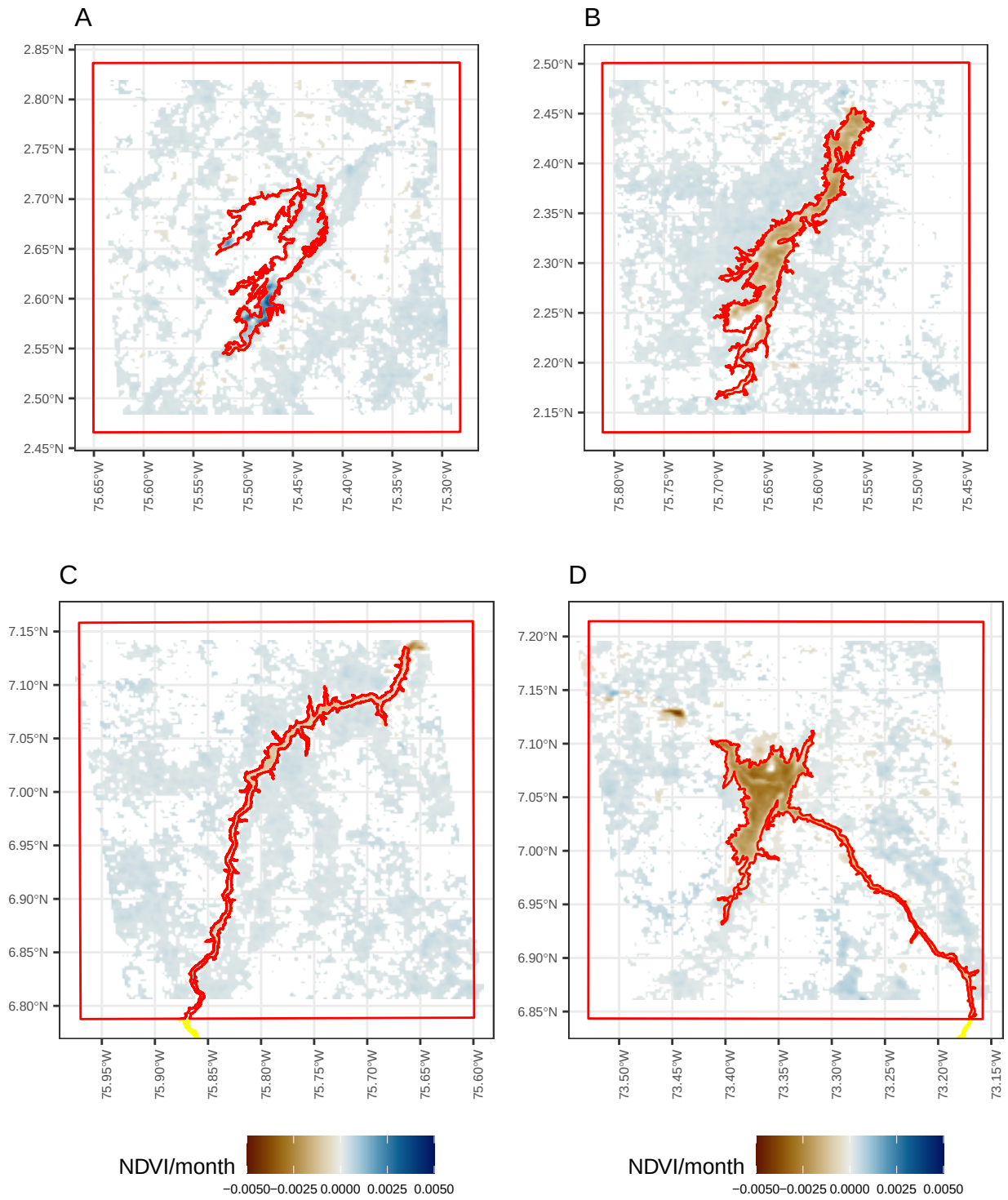


Figure 3: NDVI Spatial Mann kendall trend magnitude for each of the four reservoirs (n=266 months). Only significant trends ($P < .05$) were ploted. A. BET. B. QUI. C. ITU. D. TOP

*3.2. Changes in land surface energy balance and climatic variables*

As indicated in figure 4, differences in surface energy balance due to reservoir building and operation are most evident in the partitioning of net radiation into sensible and latent heat fluxes. More specifically, we found that Albedo ($Alb$) was different both between the spatial domains and project phases, where reservoir building produced a significant reduction in albedo in all RAs, with lower values than those detected for IAs during both phases. Changes associated with phase building correspond to $QUI - 0.07; ITU - 0.02; TOP - 0.08$. These results indicate a decrease in reflected radiation to the atmosphere in RAs ($QUI : -11.85; ITU : -2.74; TOP : -16.14 W/m^2$).

The reduction in albedo, in turn, results in increases in net radiation ($Rn$) ($QUI : 20.81; ITU : 4.07; TOP : 17.61\ W/m^2$), with exception of the ITU RA, where these changes were not significant (figure 4). These variations in Rn are also influenced by incoming radiation, which increases in TOP for the shortwave component ($TOP : 3.39\ W/m^2$) and is reduced ITU in the longwave component ($ITU : -0.41\ W/m^2$) between project phases. Similarly, longwave radiation emission changes in significatively in QUI and TOP reservoirs (figure 4), wherein QUI a reduction was detected for RA ($-7.86\ W/m^2$) and in TOP an increase in radiation emission in the IA was detected ($3.57\ W/m^2$). Despite these variations, net radiation in RAs after building did not surpass net radiation values detected in their IAs for both phases, except in the TOP reservoir.

Net radiation partitioning into latent heat flux and the sum of sensible and ground heat fluxes showed significant differences between project phases for all the reservoirs (figure 4). The reservoir building induces a significant increase in latent heat flux from the RA ($TOP : 172.55\ W/m^2$, $ITU : 200.83\ W/m^2$, $QUI : 147.96\ W/m^2$) and a subsequent reduction in sensible and ground fluxes ($TOP : -155.48\ W/m^2$; $ITU : -196.06\ W/m^2$; $QUI : -123.99\ W/m^2$). These changes produce an significant difference between the spatial domains, where latent heat for RA its higher than in IA ($TOP : 176.3\ W/m^2$; $ITU : 183.22\ W/m^2$; $QUI : 142.3\ W/m^2$; $BET : 147.51\ W/m^2$), and the sum of sensible and ground fluxes is lower ($TOP : -169.75\ W/m^2$; $ITU : -206.75\ W/m^2$; $QUI : -140.34\ W/m^2$; $BET : -134.36\ W/m^2$). Overall, these changes suggest that reservoir building and operation can increase net radiation through a reduction in albedo and also a change in longwave radiation emission, but the magnitude of these changes is one order of magnitude lower than the changes in net radiation partitioning.

During the BL phase, the monthly mean percentage of net radiation used in latent heat fluxes was $QUI : 41.0\%$, $ITU : 30.2\%$, $TOP : 38.4\%$, while in the BO phase was $QUI : 88.2\%$, $ITU : 88.6\%$, $TOP : 84.2\%$, doubling the amount of evapotranspiration in the RAs (Figure 4). However, these changes are limited to the RA, implying that in the studied reservoirs the surrounding vegetation doesn't rise its evapotranspiration due to more water availability in soil, as expected by the flooding process. The obtained variation in the annual cycle of the land surface energy balance (See figure 4), shows a regime of low variability in net radiation, which also is conditioning the low magnitude in variations of monthly heat fluxes over the RAs. This low variation can be related to the tropical conditions of the studied reservoirs.

The temporal components of incoming shortwave radiation shows no significant changes over the studied areas (Figure 4), indicating that the changes in land cover that occurred in the studied period did not generate detectable feedbacks with atmosphere that could alter the cloud regimes and the amount of shortwave incoming radiation in the scale of $1 \times 1^\circ$ (CERES measuring scale). The mean values of shortwave incoming radiation considering all cloud conditions were $170.7\ W/m^2$ for BET and QUI, $197.1\ W/m^2$ for ITU, and $209.0\ W/m^2$ for TOP. The seasonal components of this variable show a bimodal annual cycle, with maximum values of shortwave radiation during January ($+16.43\ W/m^2$) and September ($+6.77\ W/m^2$) for BET and QUI, during January ($-4.58\ W/m^2$) and August($+23.92\ W/m^2$) for ITU, and for the same months for TOP rising values of the mean radiation in these months in $+9.84\ W/m^2$ and $+12.35\ W/m^2$. The longwave radiation changed in trend only for the TOP

reservoir in two moments (8/2010 and 5/2016). Between these periods, longwave incoming radiation rises at rates of 0.11 $W/m^2$ per month, but after the second change in trend this variable decreases to $-0.15$ $W/m^2$ per month. The mean values of this variable were 369.42 $W/m^2$ for BET and QUI, 385.13 $W/m^2$ for ITU and 399.84 $W/m^2$ for TOP.

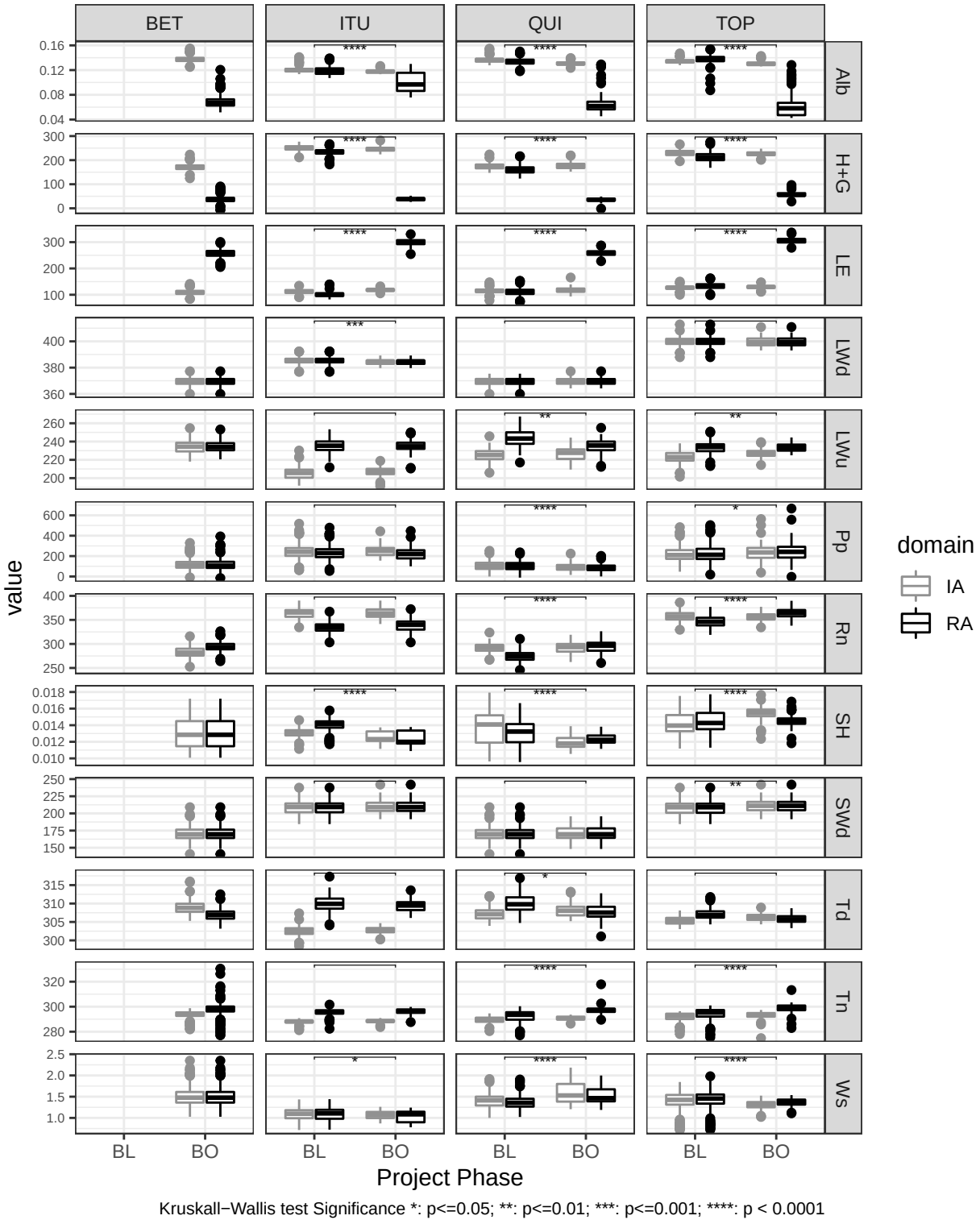


Figure 4: Changes meteorological variables for each reservoir, spatial domain and project phase. RA: Reservoir area, IA: influence area; BL: base-line, BO: Building and operation.

Due to changes in the surface, longwave radiation emission from the different reservoir areas changes based on the measured emissivity and surface temperature. We observe that emitted longwave radiation doesn't change in seasonal and trend components in any of the reservoir areas and their surroundings with exception of the TOP surroundings, where the longwave emission trend rises 7.71 $W/m^2$ and starts to decay, which changes the mean values of emission from 223.1 to 227.2 $W/m^2$. Spatially, the differences between flooded areas (RA) and land (IA) are $-0.2124$ $W/m^2$ for BET, $-8.000$ $W/m^2$ for QUI, $-27.81$ $W/m^2$ for ITU and $-6.461$ $W/m^2$ for TOP.

Using the ONI index, we found that ENSO is significantly correlated with longwave incoming radiation, due its incidence in cloud amount ($R^2 = -0.13$,$P < .05$) and cloud temperature ($R^2 = 0.07$, $P < .05$).

For latent heat, we found that there is a change in trend components on 02/2016 in the QUI reservoir surrounding area. However, for the remaining studied areas, no changes were detected. The trend component in this area rises to 138.18 $W/m^2$ (+20.65 $W/m^2$). We found that seasonal components of this variable exhibit a range between 10 and $-15$ $W/m^2$, with two maximum peaks by year, occurring in May and December. In the case of ITU the seasonal component does not show the same pattern, with only maximum value occurring by year during June. The mean values of latent heat in these regions correspond to 158.12 $W/m^2$, 118.26 $W/m^2$, 101.44 $W/m^2$ and 133.65 $W/m^2$.

Despite the observed changes in land surface energy balance partitioning, the response in meteorology did not follow the same trends. For instance, the specific humidity ($SH$) reduces in all the reservoirs and domains in the BO phase ($QUI : -8$»$10^{-4}$ $kg/kg$; $ITU : -0.0017$ $kg/kg$; $TOP : -10^{-4}$ $kg/kg$). These changes don't create a significant difference between the specific humidity between the RA and the IAs during the BO phase, in consequence the humidity reduction could be related to a more large spatial phenomena than the reservoir operation and its evaporation flux.

Similarly, wind speed ($Ws$) shows a significant variation in all the reservoirs ($QUI : 0.15$ $m/s$; $ITU : -0.05$ $m/s$; $TOP : -0.06$ $m/s$), with differences between all phases and spatial domains areas. In QUI, for example, the change in phase shows an increase in wind speed. For TOP, the wind speed values are significantly different due the phase changes and for the influence area and between the IA and the RA. Also, there were no differences between the reservoir area in BO with the Influence area during the baseline. Those results indicate that the only difference occurs in the IA during the BO phase, which is significantly lower than the differences in the other areas and phases. Although we could expect that reservoir building would induce an increase in wind speed due to the loss in surface roughness and a rise in humidity due the water availability for evaporation, the results are not consistent through all the reservoirs, highlighting the potential influence of other variables such as reservoir geometry and topography (figure 4)

Precipitation has a significant variation in QUI and TOP, which corresponds to a reduction in $QUI : -23.58$ $mm/month$ and $ITU : -22.01$ $mm/month$, and an increase in $TOP : 24.84$ $mm/month$ in the RA ($Pp$ on figure 6). Those changes can be observed in detail in the annual cycle of precipitation and air temperatures (figure 5), where during the BO phase in the case of ITU precipitation mean values reduce mainly during July and in QUI during October and April in comparison with the BL. In TOP, precipitation rises during April, September, and October.

We detected differences in daytime surface temperature ($T_d$) and night-time ($T_n$) surface temperature between IA and RA (4). During the day, surface temperature was lower in the RA, except for the ITU reservoir. This pattern, however, is reversed at night when temperatures are higher in the RA than in the IA. These variations can result from differences in heat capacity between land and water, where the water requires more energy to raise its temperature (therefore having lower values in the water body), and releases heat at a slower rate than the land (explaining higher temperatures in the

reservoir at night). Air temperature, being the mean value of night and day temperatures, becomes modulated by the night heating and the day cooling of surface due water, which explains why there its no significant changes in air temperature. These variations are also indicative of the coexistence of trend changes in atmospheric variables, as well as in land surface energy variables over the study period, discussed in the previous section.

The day time temperature shows significant differences between RA and AI in BET. Also, the RA during the baseline has higher temperature values than the IA, and the temperature observed during the BO phase in IA and RA (figure 4). For ITU a similar situation occurs where the daytime temperatures don't change between the phases, but the RA has higher temperatures (Figure 6). In TOP the day-time temperatures show that reservoir area has differences between the phase and the IA, BO the RA has higher temperatures that the IA, but after the change in phase the temperature in IA increases and in RA reduces (figure 4). In QUI, the results show that for the reservoir area, night-time temperatures did not change with the building of the reservoir (figure 4), however the temperatures of the RA are different and in fact higher than the IA in both phases, and higher in the BO phase. In ITU there were no changes in nighttime temperatures in the phase changes, and, similar to daytime temperatures, the RA exhibited higher temperatures than the IA ($4\ Tn$). Like the daytime temperatures in TOP the RA has higher temperature however during the BO the temperature rises in RA. No changes in nighttime temperatures are detected to the IA.

Air temperatures (mean value of daytime and nighttime temperatures) during the BL phase, show patterns in their annual cycle where maximum air temperatures occur in the months preceding the occurrence of maximum precipitation months. In ITU the higher air temperatures occur from December to April (figure 5). Similar patterns occur in the remaining reservoirs, however in these reservoirs precipitation and temperature show two periods of high precipitation by year, from March to May, and from September to November. In comparison with BL, during BO phase air temperature in the RA shows changes in the distribution of the hottest months through the year (Figure 7). The effects in these cases can be a response to the rises in nighttime temperatures in RAs, while in the IAs rises in temperature are presented that are not significant as was shown in figure 6.

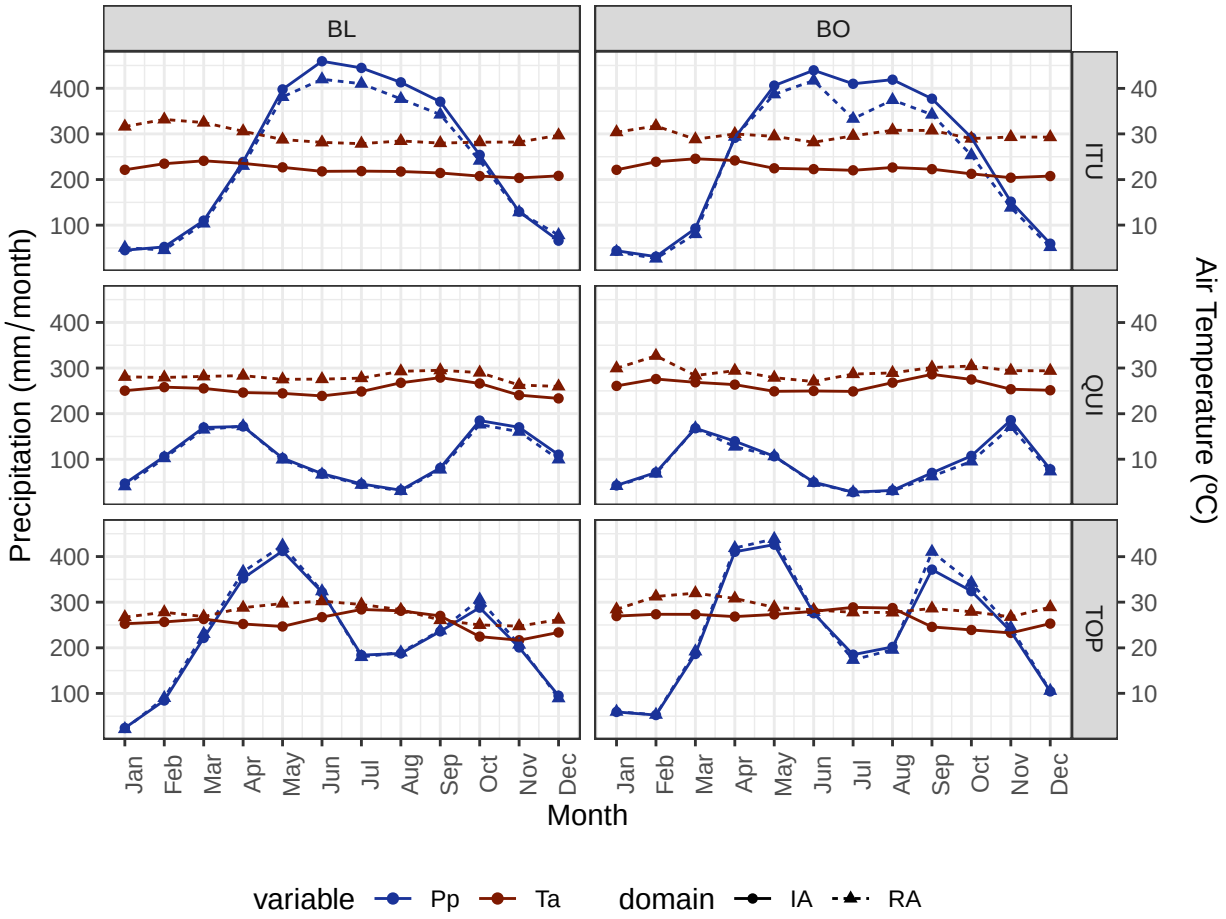


Figure 5: Changes in temperature and precipitation annual cycle for each reservoir area and project phase; BL: base-line, BO: Building and operation.

### *3.3. Relationships between land surface energy balance and atmospheric variables*

#### *3.3.1. Overall relationships*

In general, the studied variables show a high level of collinearity (Figure 6), due to the multiple interactions between the land surface energy balance, surface properties, and atmospheric processes. However, the overall correlations highlight a difference in the influence of atmospheric processes or surface properties. For example, in the studied reservoirs the surface characteristics are more determinant than the atmospheric patterns for temperature variations. Meanwhile, for precipitation, the incoming radiation (which has a low dependence on surface properties) can play a more significant role. Our results indicate that increases in evapotranspiration that follow the increases in incoming radiation can potentially induce increments in precipitation for all the studied reservoirs. Among the variables that were significantly related with (and potentially predictors of) precipitation we found albedo, shortwave radiation fluxes ($R^2 = 0.54$, $P \leq .0001$), incoming longwave radiation ($R^2 = 0.65$, $P \leq .0001$), sensible and ground heat fluxes ($R^2 = 0.32$, $P \leq .0001$), latent heat ($R^2 = 0.54$, $P \leq .0001$) and daytime temperature (to a lesser extent) ($R^2 = 0.17$, $P \leq .0001$). Also the vegetation biophysical properties are significantly correlated with the precipitation values ($LAI : R^2 = -0.22$, $P \leq .0001$, $NDVI : R^2 = 0.28$, $P \leq .0001$). Overall, out of the energy balance partitioning components, Latent heat fluxes are more strongly correlated to precipitation than sensible and ground heat fluxes.

The specific humidity of the air relates to the incoming shortwave radiation, but most importantly from long wave incoming radiation. For this variable the higher correlations were found with longwave incoming radiation ($R^2 = 0.53, P \leq .0001$), sensible and ground fluxes ($R^2 = 0.51, P \leq .0001$), while the remaining significant correlations where lower than $R^2 = 0.35$, for example shortwave incoming radiation ($R^2 = 0.27, P \leq .0001$), day time temperature ($R^2 = -0.24, P \leq .0001$) and latent heat ($R^2 = 0.21, P \leq .0001$).

Wind speed variations (obtained from GLDAS) negatively correlated with albedo values ($R^2 = -0.36, P \leq .0001$). Reductions in vegetation density and activity can induce rises in the wind speed, as indicated by the correlation between NDVI and wind speed ($R^2 = -0.20$, $P \leq .0001$). In other aspects heat fluxes (latent, sensible and ground) appear as significant predictors of the wind speed ($R^2 = -0.24$, $P \leq .0001$), however the incoming (longwave and shortwave) radiation has higher correlation values ($LWd : R^2 = -0.33$, $P \leq .0001$; $SWd : R^2 = -0.35$, $P \leq .0001$).

Day time temperatures relationship with other variables suggest a possible dependance of local surface temperatures in the surface characteristics, which modulate the emission and reflection of incoming radiation, as shown by significant correlations with albedo ($R^2 = -0.49$, $P \leq .0001$), reflected shortwave radiation ($R^2 = 0.46$, $P \leq .0001$), emitted longwave radiation ($R^2 = 0.30$, $P \leq .0001$), sensible and ground heat fluxes ($R^2 = -0.44$, $P \leq .0001$) and NDVI ($R^2 = -0.31$, $P \leq .0001$). incoming shortwave radiation is not significantly correlated with the temperature values, while the longwave incoming radiation has a low value of correlation ($SWd : R^2 = 0.005$, $P > 1$; $LWd : R^2 = -0.12$, $P \leq 0.01$).

The ENSO (indicated by the ONI index) appears to have an influence in some of the variables of land surface energy balance and meteorology in the studied reservoirs, as shown by the ONI correlation with day time temperatures ($R^2 = 0.34$, $P \leq .0001$), the longwave incoming radiation ($R^2 = 0.21$, $P \leq .0001$), latent heat ($R^2 = 0.24$, $P \leq .0001$) and also in the biophysical properties, like LAI ($R^2 = -0.28$, $P \leq .0001$).

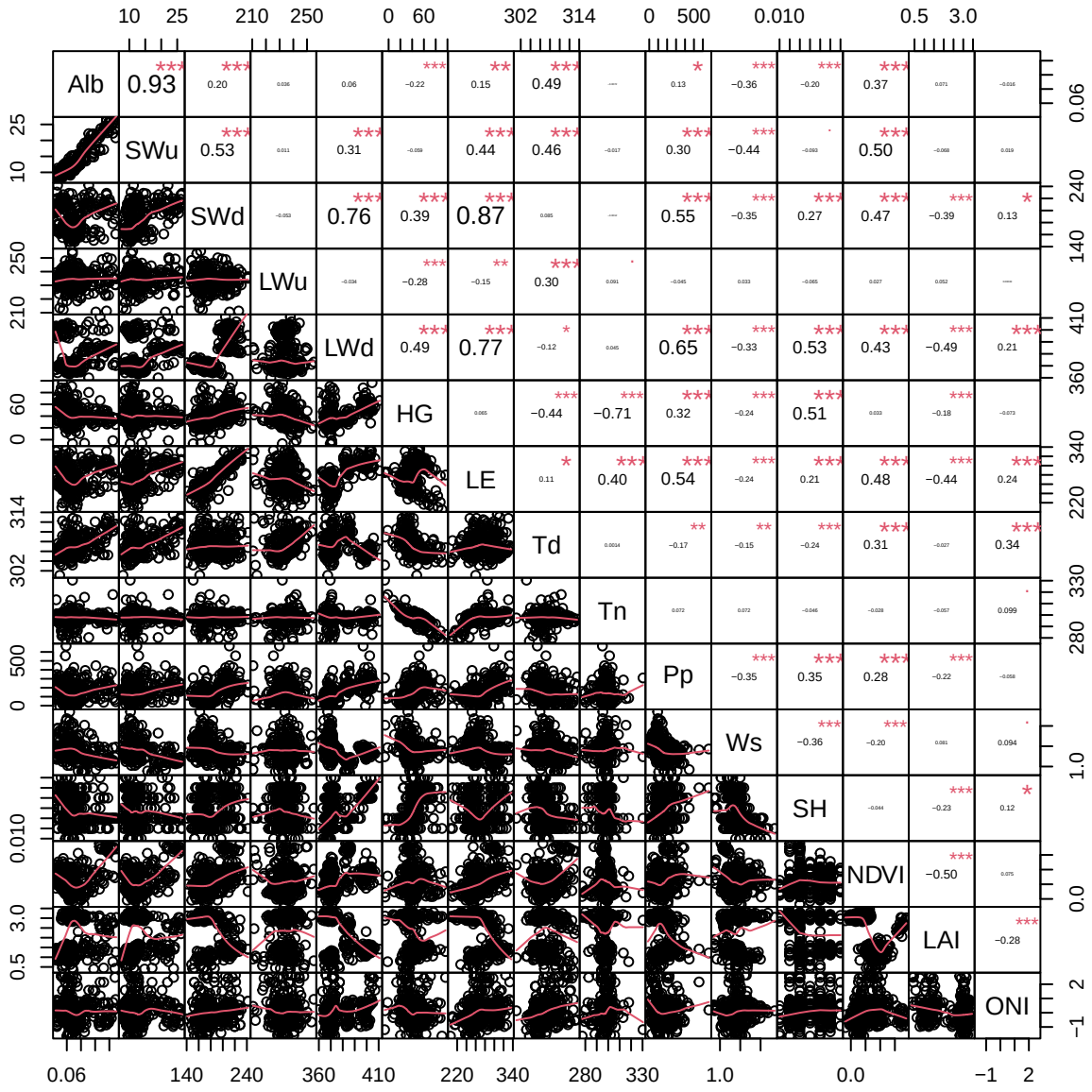


Figure 6: Correlation plots of land surface energy balance and atmospheric variables. On the bottom of the diagonal the bivariate scatter plots with a fitted line are displayed, on the top of the diagonal the value of the correlation plus the significance level as stars each significance level is associated with a symbol: ***: P $\leq$ .0001 ***: P $\leq$ .0001, **: P $\leq$ .001, *: P $\leq$ .01, .: P $\leq$ .05.

### *3.3.2. Temporal components of variation*

To improve our understanding of biophysical properties and energy budget variation consequences, we explore each of the temporal components of time series and the importance of each variable in the possible prediction of meteorological variables. In Figure 7, we show the 3 components (trend, seasonal, and remainder) of the PLS regressions adjusted for predicting precipitation, specific humidity, wind speed, diurnal day-time, and night-time temperatures. We use each of the temporal components of

predictors and outcome variables to build the regressions. Variable importance measured here is based on weighted sums of the absolute regression coefficients. The weights are a function of the reduction of the sums of squares across the number of PLS components and are computed separately for each outcome. Therefore, the contribution of the coefficients is weighted proportionally to the reduction in the sums of squares.

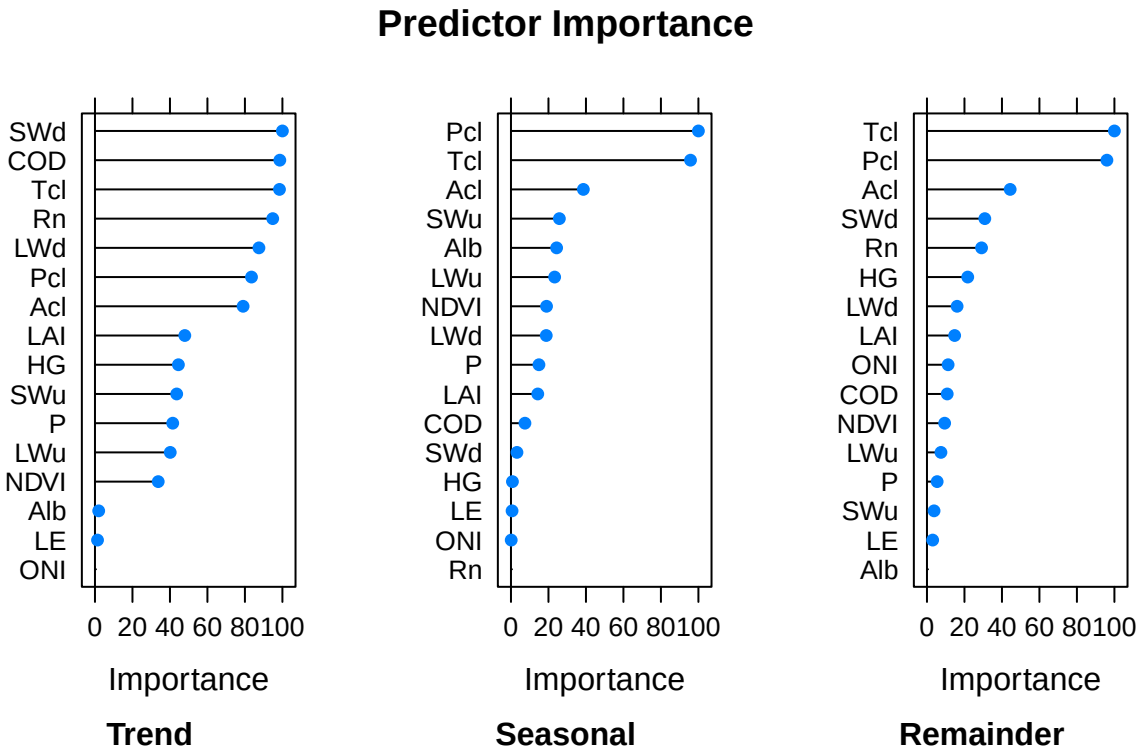


Figure 7: Importance of each variable in the prediction of the PLS outcomes in each one of the time series components.

The trends of all the variables show that with only two components of the PLS regressions, the output variables variability is explained by 94.19% while these components include 69.43% of all predictors variability. The best predicted variable is precipitation ($R^2 = 0.95, RMSE = 903.57$), followed by wind speed ($R^2 = 0.29, RMSE = 1075.11$), specific humidity ($R^2 = 0.27, RMSE = 1076.45$), day-time surface temperature ($R^2 = 0.17, RMSE = 770.19$) and night-time temperature ($R^2 = 0.0051, RMSE = 783.89$).

The most important predictor variables correspond to shortwave incoming radiation ($SW_d$), cloud optical depth ($COD$), cloud temperature ($T_{cl}$), net radiation ($Rn$), longwave incoming radiation ($LW_d$), cloud pressure ($P_{cl}$) and area ($A_{cl}$). These differences in importance across the predictor variables highlight that the observed trends in atmospheric variables are mainly related to the variation in radiation inputs on the surface, which are modulated by clouds variability, which changes the net radiation. Following the obtained importances, the surface biophysical properties like LAI and NDVI, and fluxes of radiation and heat from the surface, like sensible and ground heat fluxes, longwave radiation emission, and shortwave radiation reflection, were less important than the cloud properties and radiation inputs in the explaining of atmospheric variables trends, while the importance of albedo, latent heat, and ONI was almost null (see figure 7, Trend panel).

These results indicate that the partitioning of net radiation into sensible and ground fluxes is a better predictor of meteorological trends variability than latent heat and albedo, which are precisely the most affected variables by reservoir building and operation, in consequence, most of the observed changes in trends of the predicted atmospheric values are not directly related to the reservoir effects on land surface energy balance. Also, despite the importance of cloud patterns in the trends prediction, the ENSO (represented by the ONI index) and their shifts in magnitude and phase, are part of the least important predictors of meteorological trend values. Overall, these findings show that in the studied areas, changes in atmospheric regional-scale patterns are more important in the modulation of wind, humidity, temperatures, and precipitation than the changes associated with land cover land-use change by reservoir installation. However, surface temperatures were not explained by these variables. In this sense it is plausible that, while precipitation, wind, and humidity trends respond to atmospheric patterns, the temperature trends respond more to surface processes imposed by reservoir building.

For the seasonal components (figure 7, seasonal panel), PLS regressions can explain 85.37% of the outcomes, with a 40.97% of the predictors' variability. Seasonal variability shows reduced error in the predictions, where precipitation ($RMSE = 24.01, R^2 = 0.95$), specific humidity ($RMSE = 99.06, R^2 = 0.46$) and wind speed ($RMSE = 99.13, R^2 = 0.25$) are the best predicted variables, while surface temperatures, as with trend components, are not well predicted by the model ($T_d : RMSE = 99.43, R^2 = 0.04; T_n : RMSE = 99.13, R^2 = 0.003$). The most important predictors in this regression are associated with cloud temperature and pressure and to a minor extent the cloud area, the upward shortwave and longwave radiation fluxes, albedo, latent heat, and biophysical properties. While the incoming shortwave radiation, heat fluxes, and net radiation are not important to explain the changes in seasonal patterns of the atmospheric variables. Also, the ENSO is not an important predictor of these patterns, which is expected considering the length of this phenomenon. These results show the influence of seasonal cloud dynamics over atmospheric variables, with the participation of radiation reflection and emission from the surface, which is also related to changes in surface properties like albedo and LAI.

In consequence, the reservoir building and operation is not the most important driver of change in seasonal patterns of climate variables in the studied areas. However, it can have an effect on modulating the magnitude of these patterns due to the alteration of albedo and emissivity from the surface. Similar to the observed trend components, the surface temperatures low correlation with the predictor variables highlight that other aspects can be driving their seasonal variations. It's plausible that in this case, temperature responds better to the least important variables in the seasonal components regression, these are the heat fluxes, the incoming shortwave radiation, cloud optical depth, and net radiation.

In contrast to the other temporal components, the remaining components are not well predicted by the selected variables (figure 7, remainder panel). In fact, when using 12 components in the PLS, the variance explained for the outcome variables is only 19.49%, while covering up to 88.48% of the predictors' variability. The PLS regression has capacity to explain remainder part of variations of precipitation variability ($P_p : RMSE = 59.07$ ,$R^2 = 0.27$). However, the remaining output variables are low correlated with these regression ($q_{air} : RMSE = 30.43$, $R^2 = 0.09$; $W_s : RMSE = 30.47$, $R^2 = 0.086$; $T_d : RMSE = 30.65$, $R^2 = 0.01$; $T_n : RMSE = 30.61$, $R^2 = 0.0004$). The relative importance of the predictor variables in this regression is higher for cloud properties (temperature, pressure, and area), followed by the incoming shortwave radiation, net radiation, and the remaining fluxes of surface energy balance ($H + G$) and the longwave incoming radiation. Of lesser importance are the LAI, ONI, cloud optical depth, and NDVI, and with low importance or null importance the longwave radiation emission, air pressure, reflected shortwave radiation, latent heat, and albedo.

Overall, the remaining components show a low relationship with the predictor variables and the model itself, indicating that the variations in meteorology, outside the trend and seasonal patterns,

are not directly or significantly related to changes produced by the construction of reservoirs, like albedo reduction and latent heat rise in RA. In addition, in these remaining components the ONI may be a more relevant variable, which may be related to changes in cloud properties and precipitation variability, but not necessarily to changes in wind speed, humidity, and temperature in the studied areas.

## 4. Discussion

Our results show that reservoir building and operation in four locations in the tropical Andes impacted the vegetation structure and function. These effects are limited to the reservoir areas due to flooding, as shown by the spatial and temporal trends LAI and NDVI. In our results, Due to the spatial resolution of the data used in this analysis (250 and 500 *m per pixel*), pixels/areas flooded by the reservoir might include non-flooded areas. In these areas, vegetation could be affected by increases in the water table levels, which can relate to changes in LAI or NDVI values, as indicated by *[18, 28, 34, 10, 46]*. However, at the spatial and temporal scale of our results and analyses, there are no significant impacts on surrounding vegetation due to reservoir building.

In our results, albedo and subsequently land surface energy balance did exhibit significant changes due to reservoir building, rising the amount of monthly mean net radiation *by* $\approx 20\ Wm^{-2}$ in the reservoir area. These results are consistent with other studies *[32, 60]*. The higher impact was the variation in net radiation partitioning due to the reservoir establishment, where the latent heat, responsible for moisture fluxes to the atmosphere, comprises between 84.2% to 88.6% of net radiation in flooded areas, contrasting with land areas, where it comprises between 30.2% to 41.0%, showing a higher sensible heat flux than flooded areas. However, despite the increase in latent heat by reservoir building and operation, the precipitation and humidity don't rise in all the studied reservoirs. This observation can be related to the findings of *Zamora et al. [65]*, which highlights that in tropical and humid regions, forest areas exhibit comparable moisture fluxes with reservoirs, given that in these regions, both transpiration from land vegetation and evaporation from open water bodies are demand-driven. This means that the moisture transfer rate from the surface to the atmosphere depends on atmosphere water demand rather than on the availability of water at the surface, which would be the case in more arid regions, where the presence of reservoirs significantly altered precipitation regimes. Therefore, in humid regions, such as those included in this study, flooding (or the replacement of forests by a water body) is unlikely to create a distinctly different local climate, which differs from the effect of reservoirs in semi-arid, tundra, humid continental, and Mediterranean regions, as several studies have shown *[13, 31, 26, 14]*. In addition, cloud properties (which depend on more regional processes) were more important than land surface properties in precipitation and humidity prediction. Most of the variability in precipitation and humidity in the studied areas was not well predicted by the latent heat variations (as shown by the PLS results).

Although we combined sensible heat and ground fluxes (due to data availability) in our estimations, it is plausible that the reservoir ground heat fluxes, which represent the accumulation of heat in the water body, were higher than those in the land and thus require an independent estimation *[67]*. This would contribute to refining evaporation estimates, and potentially improve the statistical association between energy balance components and atmospheric humidity and precipitation in the studied areas. However, we hypothesize that this refinement in evapotranspiration estimates would not lead to changes in our predicted associations between reservoir installation and precipitation variability. Also, as highlighted by *Marín-Ramírez et al. [37]* advective energy fluxes, both atmospheric and hydrological, that were not explored in this work, can have a significant impact on Andean tropical reservoir surface temperature, where evaporation processes occur, that modify latent heat fluxes in a high frequency, out of the scope of our analysis (monthly periods).

In all reservoirs analyzed in this study, we identified a low impact of evapotranspiration of reservoir areas in precipitation changes. We hypothesize that despite the importance of the terrestrial processes in precipitation regimes, this can be overshadowed by the effects of larger moisture transport processes, such as oceanic moisture transport from the Atlantic and Pacific oceans. The work of *Hoyos et al. [25]* indicates that, in the northern Andes, terrestrial sources are important sources of precipitable water, with local moisture recycling only contributing to between 10% to 17% of incoming moisture, with the remaining components coming from regions like the Orinoco and Amazon Basin.

Reservoirs' morphology characteristics can be related to the direct magnitude of the changes over the land surface energy balance. ITU reservoir, for example, being a riverine reservoir has a lower impact over the evaluated components, because its extension is highly restricted to the river valley. In BET, despite being active for a larger period than the other studied reservoirs, there is no evidence of abrupt changes due to its operation. The building of a close reservoir, QUI, doesn't change in the signal of the meteorological variables, indicating a non-cumulative impact of these two reservoirs and a spatial restriction of the meteorological and biophysical changes to the flooded areas. The TOP reservoir, with a large flooded area, makes more clear the expected impacts of larger reservoirs, in which albedo drops, and the net radiation is partitioned in their most part in evapotranspiration, reducing the sensible heat flux. Also, as expected, the day and night temperatures change, principally the night temperatures in the reservoir areas, where a rise occurs by heat accumulation in the reservoir. Other studies *[68]* have suggested that the size of the reservoirs, their shape, and topographical features can play an important role in the moisture transport and the precipitation processes. These studies have suggested that the effects of reservoir characteristics on local climate are highly heterogeneous. This heterogeneity can induce opposite responses in local meteorological variables over the reservoirs and their surroundings.

## 5. Conclusions

In this work, we proposed the use of multiple tools to analyze the potential association between reservoir building and operation to the changes in surface-atmosphere exchange processes in Betania, Ituango, Quimbo, and Topocoro reservoirs in Colombia. We found that the most affected process by the abrupt change in land cover of reservoir building is the partitioning of net radiation into sensible and latent heat fluxes. These results are consistent with previous studies *[32]*.

Although reservoir building can potentially increase humidity and wind patterns due to increased availability of surface water and a reduction in surface roughness, our results indicate that these effects do not scale to changes in precipitation regimes in reservoir adjacent areas, and can be related to the high dependence of humidity and precipitation in these areas on large-scale circulation (including moisture transport from oceanic sources and larger scale continental recycling) and climatic variability in the region (including ENSO phases). However, we hypothesize that moisture generated from reservoir evaporation could potentially generate increased precipitation downwind. Future research could explore these effects using modeling techniques *[25]* or atmospheric vapor tracers *[21]*.

As expected, the largest differences in energy balance components occur between the reservoir and its surroundings, as the result of a strong change in land cover (replacing vegetation with water). However, changes in energy budgets are only restricted to the reservoir area and do not result in significant variations in temperatures and other meteorological variables in surrounding land regions. This is potentially associated with the climatic and topographical setting of these reservoirs. However, hydropower reservoir projects also produce other environmental impacts, in terms of land-use change, and ecological properties that are not assessed but complemented by our approach.

Hydropower projects can significantly alter the biophysical properties of the flooded areas, reducing the values of albedo in a way that the resultant water body reflects less shortwave radiation than land

areas. Consequently, these changes result in an increase in net radiation that is not compensated by changes in longwave radiation emission. This rise in net radiation produces changes in the flux components of the land surface energy balance, mostly resulting in increased evapotranspiration or heat accumulation in comparison to surrounding areas or the same area before the project. However, these changes do not relate or escalate to impacts in precipitation and temperature in areas close to the reservoirs.

In summary, our results suggest that, although some general patterns related to energy and radiation balances emerge from the installation of hydropower projects, their impacts on meteorological processes vary and depend on other factors such as background climate, topographical setting, land use, among others. Disentangling the mechanism behind these changes is challenging, as multiple factors can interact to produce complex responses. However, our approach, which integrates multiple statistical tools, brings an advance in evaluating the interactions between multiple input variables in the resulting climate variables over reservoirs and their influence areas, which can further complement the findings of the influences of reservoirs features in changes in the local climate. Also, this approach allows to enhance the assessment of the environmental suitability of future hydropower reservoir projects and select the best potential combination of conditions to minimize climatic impacts on surrounding areas.

## 6. References

### References


[1] Ray G Anderson, Josep G Canadell, James T Randerson, Robert B Jackson, Bruce A Hungate, Dennis D Baldocchi, George A Ban-Weiss, Gordon B Bonan, Ken Caldeira, Long Cao, Noah S Diffenbaugh, Kevin R Gurney, Lara M Kueppers, Beverly E Law, Sebastiaan Luyssaert, and Thomas L O'Halloran. Biophysical considerations in forestry for climate protection. *Frontiers in Ecology and the Environment*, 9(3):174–182, April 2011. ISSN 1540-9295, 1540-9309. doi: 10.1890/090179. URL `https://onlinelibrary.wiley.com/doi/abs/10.1890/090179`.

[2] Kristina J. Anderson-Teixeira, Peter K. Snyder, Tracy E. Twine, Santiago V. Cuadra, Marcos H. Costa, and Evan H. DeLucia. Climate-regulation services of natural and agricultural ecoregions of the Americas. *Nature Climate Change*, 2(3):177–181, March 2012. ISSN 1758-678X, 1758-6798. doi: 10.1038/nclimate1346. URL `http://www.nature.com/articles/nclimate1346`.

[3] Jushan Bai and Pierre Perron. Computation and analysis of multiple structural change models. *Journal of Applied Econometrics*, 18(1):1–22, January 2003. ISSN 0883-7252, 1099-1255. doi: 10.1002/jae.659. URL `https://onlinelibrary.wiley.com/doi/10.1002/jae.659`.

[4] D. Baldocchi. Ecosystem Services of Energy Exchange and Regulation. In *Climate Vulnerability*, pages 81–92. Elsevier, 2013. ISBN 978-0-12-384704-1. doi: 10.1016/B978-0-12-384703-4.00410-X. URL `https://linkinghub.elsevier.com/retrieve/pii/B978012384703400410X`.

[5] Dennis Baldocchi. Measuring fluxes of trace gases and energy between ecosystems and the atmosphere - the state and future of the eddy covariance method. *Global Change Biology*, 20(12):3600–3609, December 2014. ISSN 13541013. doi: 10.1111/gcb.12649. URL `https://onlinelibrary.wiley.com/doi/10.1111/gcb.12649`.

[6] Alan K. Betts, Ahmed B. Tawfik, and Raymond L. Desjardins. Revisiting Hydrometeorology Using Cloud and Climate Observations. *Journal of Hydrometeorology*, 18(4):939–955, April 2017. ISSN 1525-755X, 1525-7541. doi: 10.1175/JHM-D-16-0203.1. URL `http://journals.ametsoc.org/doi/10.1175/JHM-D-16-0203.1`.

[7] G. B. Bonan. Forests and Climate Change: Forcings, Feedbacks, and the Climate Benefits of Forests. *Science*, 320(5882):1444–1449, June 2008. ISSN 0036-8075, 1095-9203. doi: 10.1126/science.1155121. URL https://www.sciencemag.org/lookup/doi/10.1126/science.1155121.

[8] Isobel Bramer, Barbara J. Anderson, Jonathan Bennie, Andrew J. Bladon, Pieter De Frenne, Deborah Hemming, Ross A. Hill, Michael R. Kearney, Christian Körner, Amanda H. Korstjens, Jonathan Lenoir, Ilya M.D. Maclean, Christopher D. Marsh, Michael D. Morecroft, Ralf Ohlemüller, Helen D. Slater, Andrew J. Suggitt, Florian Zellweger, and Phillipa K. Gillingham. Advances in Monitoring and Modelling Climate at Ecologically Relevant Scales. In *Advances in Ecological Research*, volume 58, pages 101–161. Elsevier, 2018. ISBN 978-0-12-813949-3. doi: 10.1016/bs.aecr.2017.12.005. URL https://linkinghub.elsevier.com/retrieve/pii/S0065250417300302.

[9] N. A. Brunsell, D. B. Mechem, and M. C. Anderson. Surface heterogeneity impacts on boundary layer dynamics via energy balance partitioning. *Atmospheric Chemistry and Physics*, 11 (7):3403–3416, April 2011. ISSN 1680-7324. doi: 10.5194/acp-11-3403-2011. URL https://acp.copernicus.org/articles/11/3403/2011/.

[10] Gang Chen, Ryan P. Powers, Luis M.T. de Carvalho, and Brice Mora. Spatiotemporal patterns of tropical deforestation and forest degradation in response to the operation of the Tucuruí hydroelectric dam in the Amazon basin. *Applied Geography*, 63:1–8, September 2015. ISSN 01436228. doi: 10.1016/j.apgeog.2015.06.001. URL https://linkinghub.elsevier.com/retrieve/pii/S0143622815001368.

[11] Robert B. Cleveland, William S. Cleveland, Jean E. McRae, and Irma Terpenning. STL: A Seasonal-Trend Decomposition Procedure Based on Loess (with Discussion). *Journal of Official Statistics*, 6, 1990.

[12] Edouard L. Davin and Nathalie de Noblet-Ducoudré. Climatic Impact of Global-Scale Deforestation: Radiative versus Nonradiative Processes. *Journal of Climate*, 23(1):97–112, January 2010. ISSN 1520-0442, 0894-8755. doi: 10.1175/2009JCLI3102.1. URL http://journals.ametsoc.org/doi/10.1175/2009JCLI3102.1.

[13] Ahmed Mohamed Degu, Faisal Hossain, Dev Niyogi, Roger Pielke, J. Marshall Shepherd, Nathalie Voisin, and Themis Chronis. The influence of large dams on surrounding climate and precipitation patterns: DAMS AND LOCAL CLIMATE. *Geophysical Research Letters*, 38(4):n/a–n/a, February 2011. ISSN 00948276. doi: 10.1029/2010GL046482. URL http://doi.wiley.com/10.1029/2010GL046482.

[14] Georgia Destouni, Fernando Jaramillo, and Carmen Prieto. Hydroclimatic shifts driven by human water use for food and energy production. *Nature Climate Change*, 3(3):213–217, March 2013. ISSN 1758-678X, 1758-6798. doi: 10.1038/nclimate1719. URL http://www.nature.com/articles/nclimate1719.

[15] Paul A. Dirmeyer and Subhadeep Halder. Sensitivity of Numerical Weather Forecasts to Initial Soil Moisture Variations in CFSv2. *Weather and Forecasting*, 31(6):1973–1983, December 2016. ISSN 0882-8156, 1520-0434. doi: 10.1175/WAF-D-16-0049.1. URL https://journals.ametsoc.org/doi/10.1175/WAF-D-16-0049.1.

[16] Alexander Dokumentov and Rob J. Hyndman. STR: Seasonal-Trend Decomposition Using Regression, June 2021. URL http://arxiv.org/abs/2009.05894. Number: arXiv:2009.05894 arXiv:2009.05894 [stat].

[17] Gregory Duveiller, Josh Hooker, and Alessandro Cescatti. The mark of vegetation change on Earth's surface energy balance. *Nature Communications*, 9(1):679, December 2018. ISSN 2041-1723. doi: 10.1038/s41467-017-02810-8. URL http://www.nature.com/articles/s41467-017-02810-8.

[18] Leandro Valle Ferreira, Denise A. Cunha, Priscilla P. Chaves, Darley C.L. Matos, and Pia Parolin. Impacts of hydroelectric dams on alluvial riparian plant communities in eastern Brazilian Amazonian. *Anais da Academia Brasileira de Ciências*, 85(3):1013–1023, September 2013. ISSN 0001-3765. doi: 10.1590/S0001-37652013000300012. URL http://www.scielo.br/scielo.php?script=sci_arttext&pid=S0001-37652013000301013&lng=en&tlng=en.

[19] Matt Finer and Clinton N. Jenkins. Proliferation of Hydroelectric Dams in the Andean Amazon and Implications for Andes-Amazon Connectivity. *PLoS ONE*, 7(4):e35126, April 2012. ISSN 1932-6203. doi: 10.1371/journal.pone.0035126. URL https://dx.plos.org/10.1371/journal.pone.0035126.

[20] Pierre Gentine, Adam Massmann, Benjamin R. Lintner, Sayed Hamed Alemohammad, Rong Fu, Julia K. Green, Daniel Kennedy, and Jordi Vilà-Guerau de Arellano. Land–atmosphere interactions in the tropics. preprint, Global hydrology/Remote Sensing and GIS, February 2019. URL https://hess.copernicus.org/preprints/hess-2019-12/hess-2019-12.pdf.

[21] H. F. Goessling and C. H. Reick. Atmospheric water vapour tracers and the significance of the vertical dimension. preprint, Hydrosphere Interactions/Atmospheric Modelling/Troposphere/Physics (physical properties and processes), November 2012. URL https://acp.copernicus.org/preprints/12/30119/2012/acpd-12-30119-2012.pdf.

[22] B. P. Guillod, B. Orlowsky, D. Miralles, A. J. Teuling, P. Blanken, N. Buchmann, P. Ciais, M. Ek, K. L. Findell, P. Gentine, B. R. Lintner, R. L. Scott, B. Van den Hurk, and S. I. Seneviratne. Land surface controls on afternoon precipitation diagnosed from observational data: uncertainties, confounding factors and the possible role of vegetation interception. preprint, Clouds and Precipitation/Remote Sensing/Troposphere/Physics (physical properties and processes), November 2013. URL https://acp.copernicus.org/preprints/13/29137/2013/acpd-13-29137-2013.pdf.

[23] M. Hirschi, B. Mueller, W. Dorigo, and S.I. Seneviratne. Using remotely sensed soil moisture for land–atmosphere coupling diagnostics: The role of surface vs. root-zone soil moisture variability. *Remote Sensing of Environment*, 154:246–252, November 2014. ISSN 00344257. doi: 10.1016/j.rse.2014.08.030. URL https://linkinghub.elsevier.com/retrieve/pii/S003442571400337X.

[24] Faisal Hossain, Ahmed M. Degu, Wondmagegn Yigzaw, Steve Burian, Dev Niyogi, James Marshall Shepherd, and Roger Pielke. Climate Feedback–Based Provisions for Dam Design, Operations, and Water Management in the 21st Century. *Journal of Hydrologic Engineering*, 17(8):837–850, August 2012. ISSN 1084-0699, 1943-5584. doi: 10.1061/(ASCE)HE.1943-5584.0000541. URL http://ascelibrary.org/doi/10.1061/%28ASCE%29HE.1943-5584.0000541.

[25] I. Hoyos, F. Dominguez, J. Cañón-Barriga, J. A. Martínez, R. Nieto, L. Gimeno, and P. A. Dirmeyer. Moisture origin and transport processes in Colombia, northern South America. *Climate Dynamics*, 50(3-4):971–990, February 2018. ISSN 0930-7575, 1432-0894. doi: 10.1007/s00382-017-3653-6. URL http://link.springer.com/10.1007/s00382-017-3653-6.

[26] Fernando Jaramillo and Georgia Destouni. Comment on "Planetary boundaries: Guiding human development on a changing planet". *Science*, 348(6240):1217–1217, June 2015. ISSN 0036-8075, 1095-9203. doi: 10.1126/science.aaa9629. URL https://www.science.org/doi/10.1126/science.aaa9629.

[27] Pedro A. Jimenez, Jordi Vila-Guerau de Arellano, Jorge Navarro, and J. Fidel Gonzalez-Rouco. Understanding Land–Atmosphere Interactions across a Range of Spatial and Temporal Scales. *Bulletin of the American Meteorological Society*, 95(1):ES14–ES17, January 2014. ISSN 0003-0007, 1520-0477. doi: 10.1175/BAMS-D-13-00029.1. URL http://journals.ametsoc.org/doi/10.1175/BAMS-D-13-00029.1.

[28] Julia Jones, Auro Almeida, Felipe Cisneros, Andres Iroumé, Esteban Jobbágy, Antonio Lara, Walter de Paula Lima, Christian Little, Carlos Llerena, Luis Silveira, and Juan Camilo Villegas. Forests and water in South America: Forests and water in South America. *Hydrological Processes*, 31(5):972–980, February 2017. ISSN 08856087. doi: 10.1002/hyp.11035. URL https://onlinelibrary.wiley.com/doi/10.1002/hyp.11035.

[29] Randal D. Koster and Sarith P. P. Mahanama. Land Surface Controls on Hydroclimatic Means and Variability. *Journal of Hydrometeorology*, 13(5):1604–1620, October 2012. ISSN 1525-755X, 1525-7541. doi: 10.1175/JHM-D-12-050.1. URL http://journals.ametsoc.org/doi/10.1175/JHM-D-12-050.1.

[30] B.E Law, E Falge, L Gu, D.D Baldocchi, P Bakwin, P Berbigier, K Davis, A.J Dolman, M Falk, J.D Fuentes, A Goldstein, A Granier, A Grelle, D Hollinger, I.A Janssens, P Jarvis, N.O Jensen, G Katul, Y Mahli, G Matteucci, T Meyers, R Monson, W Munger, W Oechel, R Olson, K Pilegaard, K.T Paw U, H Thorgeirsson, R Valentini, S Verma, T Vesala, K Wilson, and S Wofsy. Environmental controls over carbon dioxide and water vapor exchange of terrestrial vegetation. *Agricultural and Forest Meteorology*, 113(1-4):97–120, December 2002. ISSN 01681923. doi: 10.1016/S0168-1923(02)00104-1. URL https://linkinghub.elsevier.com/retrieve/pii/S0168192302001041.

[31] Lea Levi, Fernando Jaramillo, Roko Andričević, and Georgia Destouni. Hydroclimatic changes and drivers in the Sava River Catchment and comparison with Swedish catchments. *Ambio*, 44 (7):624–634, November 2015. ISSN 0044-7447, 1654-7209. doi: 10.1007/s13280-015-0641-0. URL http://link.springer.com/10.1007/s13280-015-0641-0.

[32] Scott R. Loarie, David B. Lobell, Gregory P. Asner, and Christopher B. Field. Land-Cover and Surface Water Change Drive Large Albedo Increases in South America*. *Earth Interactions*, 15 (7):1–16, February 2011. ISSN 1087-3562. doi: 10.1175/2010EI342.1. URL https://journals.ametsoc.org/doi/10.1175/2010EI342.1.

[33] Norman G. Loeb, David R. Doelling, Hailan Wang, Wenying Su, Cathy Nguyen, Joseph G. Corbett, Lusheng Liang, Cristian Mitrescu, Fred G. Rose, and Seiji Kato. Clouds and the Earth's Radiant Energy System (CERES) Energy Balanced and Filled (EBAF) Top-of-Atmosphere (TOA) Edition-4.0 Data Product. *Journal of Climate*, 31(2):895–918, January 2018. ISSN 0894-8755, 1520-0442. doi: 10.1175/JCLI-D-17-0208.1. URL https://journals.ametsoc.org/doi/10.1175/JCLI-D-17-0208.1.

[34] Sf Lopes, Vs Vale, Ja Prado Júnior, and I Schiavini. Impacts of artificial reservoirs on floristic diversity and plant functional traits in dry forests after 15 years. *Brazilian Journal of Biology*, 75(3):548–557, September 2015. ISSN 1678-4375, 1519-6984. doi: 10.1590/1519-6984.16013. URL http://www.scielo.br/scielo.php?script=sci_arttext&pid=S1519-69842015000400548&lng=en&tlng=en.

[35] Hsi-Yen Ma, C. Roberto Mechoso, Yongkang Xue, Heng Xiao, J. David Neelin, and Xuan Ji. On the Connection between Continental-Scale Land Surface Processes and the Tropical Climate in a Coupled Ocean–Atmosphere–Land System. *Journal of Climate*, 26(22):9006–9025, November 2013. ISSN 0894-8755, 1520-0442. doi: 10.1175/JCLI-D-12-00819.1. URL http://journals.ametsoc.org/doi/10.1175/JCLI-D-12-00819.1.

[36] Rezaul Mahmood, Roger A. Pielke, Kenneth G. Hubbard, Dev Niyogi, Paul A. Dirmeyer, Clive McAlpine, Andrew M. Carleton, Robert Hale, Samuel Gameda, Adriana Beltrán-Przekurat, Bruce Baker, Richard McNider, David R. Legates, Marshall Shepherd, Jinyang Du, Peter D. Blanken, Oliver W. Frauenfeld, U.S. Nair, and Souleymane Fall. Land cover changes and their biogeophysical effects on climate: LAND COVER CHANGES AND THEIR BIOGEOPHYSICAL EFFECTS

ON CLIMATE. *International Journal of Climatology*, 34(4):929–953, March 2014. ISSN 08998418. doi: 10.1002/joc.3736. URL https://onlinelibrary.wiley.com/doi/10.1002/joc.3736.

[37] Arlex Marín-Ramírez, Andrés Gómez-Giraldo, and Ricardo Román-Botero. Variación estacional de la temperatura media y los flujos advectivos y atmosféricos de calor en un embalse tropical andino. *Revista de la Academia Colombiana de Ciencias Exactas, Físicas y Naturales*, 44(171): 360–375, June 2020. ISSN 2382-4980, 0370-3908. doi: 10.18257/raccefyn.1081. URL https://raccefyn.co/index.php/raccefyn/article/view/1081.

[38] D.L. McJannet, I.T. Webster, and F.J. Cook. An area-dependent wind function for estimating open water evaporation using land-based meteorological data. *Environmental Modelling & Software*, 31:76–83, May 2012. ISSN 13648152. doi: 10.1016/j.envsoft.2011.11.017. URL https://linkinghub.elsevier.com/retrieve/pii/S1364815211002805.

[39] Diego G. Miralles, Adriaan J. Teuling, Chiel C. van Heerwaarden, and Jordi Vilà-Guerau de Arellano. Mega-heatwave temperatures due to combined soil desiccation and atmospheric heat accumulation. *Nature Geoscience*, 7(5):345–349, May 2014. ISSN 1752-0894, 1752-0908. doi: 10.1038/ngeo2141. URL http://www.nature.com/articles/ngeo2141.

[40] Emilio F. Moran, Maria Claudia Lopez, Nathan Moore, Norbert Müller, and David W. Hyndman. Sustainable hydropower in the 21st century. *Proceedings of the National Academy of Sciences*, 115(47):11891–11898, November 2018. ISSN 0027-8424, 1091-6490. doi: 10.1073/pnas.1809426115. URL http://www.pnas.org/lookup/doi/10.1073/pnas.1809426115.

[41] Debasish PaiMazumder and James M. Done. Potential predictability sources of the 2012 U.S. drought in observations and a regional model ensemble. *Journal of Geophysical Research: Atmospheres*, 121(21):12,581–12,592, November 2016. ISSN 2169-897X, 2169-8996. doi: 10.1002/2016JD025322. URL https://onlinelibrary.wiley.com/doi/abs/10.1002/2016JD025322.

[42] M. C. Peel, B. L. Finlayson, and T. A. McMahon. Updated world map of the Köppen-Geiger climate classification. *Hydrology and Earth System Sciences*, 11(5):1633–1644, October 2007. ISSN 1607-7938. doi: 10.5194/hess-11-1633-2007. URL https://hess.copernicus.org/articles/11/1633/2007/.

[43] M. Potes, R. Salgado, M. J. Costa, M. Morais, D. Bortoli, I. Kostadinov, and I. Mammarella. Lake–atmosphere interactions at Alqueva reservoir: a case study in the summer of 2014. *Tellus A: Dynamic Meteorology and Oceanography*, 69(1):1272787, January 2017. ISSN 1600-0870. doi: 10.1080/16000870.2016.1272787. URL https://www.tandfonline.com/doi/full/10.1080/16000870.2016.1272787.

[44] Joshua K. Roundy, Craig R. Ferguson, and Eric F. Wood. Temporal Variability of Land–Atmosphere Coupling and Its Implications for Drought over the Southeast United States. *Journal of Hydrometeorology*, 14(2):622–635, April 2013. ISSN 1525-755X, 1525-7541. doi: 10.1175/JHM-D-12-090.1. URL http://journals.ametsoc.org/doi/10.1175/JHM-D-12-090.1.

[45] Joseph A. Santanello, Paul A. Dirmeyer, Craig R. Ferguson, Kirsten L. Findell, Ahmed B. Tawfik, Alexis Berg, Michael Ek, Pierre Gentine, Benoit P. Guillod, Chiel van Heerwaarden, Joshua Roundy, and Volker Wulfmeyer. Land–Atmosphere Interactions: The LoCo Perspective. *Bulletin of the American Meteorological Society*, 99(6):1253–1272, June 2018. ISSN 0003-0007, 1520-0477. doi: 10.1175/BAMS-D-17-0001.1. URL https://journals.ametsoc.org/view/journals/bams/99/6/bams-d-17-0001.1.xml.

[46] Vagner Santiago do Vale, Ana Paula De Oliveira, Jamir Afonso Do Prado-Junior, Patrícia Ribeiro Londe, and Diego Raymundo Nascimento. Damming water influences the structure, composition and functions of adjacent savannahs. *Madera y Bosques*, 23(1), March 2017. ISSN 2448-7597, 1405-0471. doi: 10.21829/myb.2017.2311527. URL http://myb.ojs.inecol.mx/index.php/myb/article/view/1527.

[47] W. James Shuttleworth. *Terrestrial hydrometeorology*. Wiley-Blackwell, Hoboken, N.J, 2012. ISBN 978-0-470-65938-0 978-0-470-65937-3. OCLC: ocn746834701.

[48] Adriaan J. Teuling, Christopher M. Taylor, Jan Fokke Meirink, Lieke A. Melsen, Diego G. Miralles, Chiel C. van Heerwaarden, Robert Vautard, Annemiek I. Stegehuis, Gert-Jan Nabuurs, and Jordi Vilà-Guerau de Arellano. Observational evidence for cloud cover enhancement over western European forests. *Nature Communications*, 8(1):14065, April 2017. ISSN 2041-1723. doi: 10.1038/ncomms14065. URL http://www.nature.com/articles/ncomms14065.

[49] P. A. Troch, G. Carrillo, M. Sivapalan, T. Wagener, and K. Sawicz. Climate-vegetation-soil interactions and long-term hydrologic partitioning: signatures of catchment co-evolution. *Hydrology and Earth System Sciences*, 17(6):2209–2217, June 2013. ISSN 1607-7938. doi: 10.5194/hess-17-2209-2013. URL https://hess.copernicus.org/articles/17/2209/2013/.

[50] J.G. Tundisi, J. Goldemberg, T. Matsumura-Tundisi, and A.C.F. Saraiva. How many more dams in the Amazon? *Energy Policy*, 74:703–708, November 2014. ISSN 03014215. doi: 10.1016/j.enpol.2014.07.013. URL https://linkinghub.elsevier.com/retrieve/pii/S0301421514004170.

[51] Vagner S Vale, I Schiavini, J A Prado-júnior, Ana P Oliveira, and André E Gusson. Rapid changes in tree composition and biodiversity: consequences of dams on dry seasonal forests. *Revista Chilena de Historia Natural*, 88(1):13, December 2015. ISSN 0717-6317. doi: 10.1186/s40693-015-0043-5. URL http://www.revchilhistnat.com/content/88/1/13.

[52] Albert I.J.M. van Dijk, John H. Gash, Eva van Gorsel, Peter D. Blanken, Alessandro Cescatti, Carmen Emmel, Bert Gielen, Ian N. Harman, Gerard Kiely, Lutz Merbold, Leonardo Montagnani, Eddy Moors, Matteo Sottocornola, Andrej Varlagin, Christopher A. Williams, and Georg Wohlfahrt. Rainfall interception and the coupled surface water and energy balance. *Agricultural and Forest Meteorology*, 214-215:402–415, December 2015. ISSN 01681923. doi: 10.1016/j.agrformet.2015.09.006. URL https://linkinghub.elsevier.com/retrieve/pii/S016819231500711X.

[53] Jan Verbesselt, Rob Hyndman, Glenn Newnham, and Darius Culvenor. Detecting trend and seasonal changes in satellite image time series. *Remote Sensing of Environment*, 114(1):106–115, January 2010. ISSN 00344257. doi: 10.1016/j.rse.2009.08.014. URL https://linkinghub.elsevier.com/retrieve/pii/S003442570900265X.

[54] Kaicun Wang. Estimation of surface long wave radiation and broadband emissivity using Moderate Resolution Imaging Spectroradiometer (MODIS) land surface temperature/emissivity products. *Journal of Geophysical Research*, 110(D11):D11109, 2005. ISSN 0148-0227. doi: 10.1029/2004JD005566. URL http://doi.wiley.com/10.1029/2004JD005566.

[55] S.-Y. Simon Wang, Joseph Santanello, Hailan Wang, Daniel Barandiaran, Rachel T. Pinker, Siegfried Schubert, Robert R. Gillies, Robert Oglesby, Kyle Hilburn, Ayse Kilic, and Paul Houser. An intensified seasonal transition in the Central U.S. that enhances summer drought. *Journal of Geophysical Research: Atmospheres*, 120(17):8804–8816, September 2015. ISSN 2169-897X, 2169-8996. doi: 10.1002/2014JD023013. URL https://onlinelibrary.wiley.com/doi/abs/10.1002/2014JD023013.

[56] Zhuosen Wang, Crystal B. Schaaf, Qingsong Sun, JiHyun Kim, Angela M. Erb, Feng Gao, Miguel O. Román, Yun Yang, Shelley Petroy, Jeffrey R. Taylor, Jeffrey G. Masek, Jeffrey T. Morisette, Xiaoyang Zhang, and Shirley A. Papuga. Monitoring land surface albedo and vegetation dynamics using high spatial and temporal resolution synthetic time series from Landsat and the MODIS BRDF/NBAR/albedo product. *International Journal of Applied Earth Observation and Geoinformation*, 59:104–117, July 2017. ISSN 03032434. doi: 10.1016/j.jag.2017.03.008. URL https://linkinghub.elsevier.com/retrieve/pii/S0303243417300715.

[57] Robert G. Wetzel. *Limnology: Lake And River Ecosystem*. 3 edition, 2011. ISBN 978-0-12-744760-5.

[58] Christopher A. Williams, Markus Reichstein, Nina Buchmann, Dennis Baldocchi, Christian Beer, Christopher Schwalm, Georg Wohlfahrt, Natalia Hasler, Christian Bernhofer, Thomas Foken, Dario Papale, Stan Schymanski, and Kevin Schaefer. Climate and vegetation controls on the surface water balance: Synthesis of evapotranspiration measured across a global network of flux towers: CLIMATE AND VEGETATION CONTROLS ON SURFACE WATER BALANCE. *Water Resources Research*, 48(6), June 2012. ISSN 00431397. doi: 10.1029/2011WR011586. URL http://doi.wiley.com/10.1029/2011WR011586.

[59] Jesse Winchester, Rezaul Mahmood, William Rodgers, Faisal Hossain, Eric Rappin, Joshua Durkee, and Themis Chronis. A Model-Based Assessment of Potential Impacts of Man-Made Reservoirs on Precipitation. *Earth Interactions*, 21(9):1–31, September 2017. ISSN 1087-3562. doi: 10.1175/EI-D-16-0016.1. URL https://journals.ametsoc.org/doi/10.1175/EI-D-16-0016.1.

[60] Georg Wohlfahrt, Enrico Tomelleri, and Albin Hammerle. The albedo–climate penalty of hydropower reservoirs. *Nature Energy*, 6(4):372–377, April 2021. ISSN 2058-7546. doi: 10.1038/s41560-021-00784-y. URL http://www.nature.com/articles/s41560-021-00784-y.

[61] Abel T. Woldemichael, Faisal Hossain, Roger Pielke, and Adriana Beltrán-Przekurat. Understanding the impact of dam-triggered land use/land cover change on the modification of extreme precipitation. *Water Resources Research*, 48(9):2011WR011684, September 2012. ISSN 0043-1397, 1944-7973. doi: 10.1029/2011WR011684. URL https://onlinelibrary.wiley.com/doi/10.1029/2011WR011684.

[62] Volker Wulfmeyer, David D. Turner, B. Baker, R. Banta, A. Behrendt, T. Bonin, W. A. Brewer, M. Buban, A. Choukulkar, E. Dumas, R. M. Hardesty, T. Heus, J. Ingwersen, D. Lange, T. R. Lee, S. Metzendorf, S. K. Muppa, T. Meyers, R. Newsom, M. Osman, S. Raasch, J. Santanello, C. Senff, F. Späth, T. Wagner, and T. Weckwerth. A New Research Approach for Observing and Characterizing Land–Atmosphere Feedback. *Bulletin of the American Meteorological Society*, 99(8):1639–1667, August 2018. ISSN 0003-0007, 1520-0477. doi: 10.1175/BAMS-D-17-0009.1. URL https://journals.ametsoc.org/view/journals/bams/99/8/bams-d-17-0009.1.xml.

[63] Yongkang Xue, Fernando De Sales, Ratko Vasic, C. Roberto Mechoso, Akio Arakawa, and Stephen Prince. Global and Seasonal Assessment of Interactions between Climate and Vegetation Biophysical Processes: A GCM Study with Different Land–Vegetation Representations. *Journal of Climate*, 23(6):1411–1433, March 2010. ISSN 1520-0442, 0894-8755. doi: 10.1175/2009JCLI3054.1. URL http://journals.ametsoc.org/doi/10.1175/2009JCLI3054.1.

[64] Wondmagegn Yigzaw, Faisal Hossain, and Alfred Kalyanapu. Impact of Artificial Reservoir Size and Land Use/Land Cover Patterns on Probable Maximum Precipitation and Flood: Case of Folsom Dam on the American River. *Journal of Hydrologic Engineering*, 18(9):1180–1190, September 2013. ISSN 1084-0699, 1943-5584. doi: 10.1061/(ASCE)HE.1943-5584.0000722. URL http://ascelibrary.org/doi/10.1061/%28ASCE%29HE.1943-5584.0000722.

[65] David Zamora, Erasmo Rodríguez, and Fernando Jaramillo. Hydroclimatic Effects of a Hydropower Reservoir in a Tropical Hydrological Basin. *Sustainability*, 12(17):6795, August 2020. ISSN 2071-1050. doi: 10.3390/su12176795. URL https://www.mdpi.com/2071-1050/12/17/6795.

[66] Christiane Zarfl, Alexander E. Lumsdon, Jürgen Berlekamp, Laura Tydecks, and Klement Tockner. A global boom in hydropower dam construction. *Aquatic Sciences*, 77(1):161–170, January 2015. ISSN 1015-1621, 1420-9055. doi: 10.1007/s00027-014-0377-0. URL http://link.springer.com/10.1007/s00027-014-0377-0.

[67] Gang Zhao, Huilin Gao, and Ximing Cai. Estimating lake temperature profile and evaporation losses by leveraging MODIS LST data. *Remote Sensing of Environment*, 251:112104, December 2020. ISSN 00344257. doi: 10.1016/j.rse.2020.112104. URL https://linkinghub.elsevier.com/retrieve/pii/S0034425720304776.

[68] Yiyang Zhao, Suning Liu, and Haiyun Shi. Impacts of dams and reservoirs on local climate change: a global perspective. *Environmental Research Letters*, 16(10):104043, October 2021. ISSN 1748-9326. doi: 10.1088/1748-9326/ac263c. URL https://iopscience.iop.org/article/10.1088/1748-9326/ac263c.

[69] Tian Zhou, Bart Nijssen, Huilin Gao, and Dennis P. Lettenmaier. The Contribution of Reservoirs to Global Land Surface Water Storage Variations*. *Journal of Hydrometeorology*, 17(1):309–325, January 2016. ISSN 1525-755X, 1525-7541. doi: 10.1175/JHM-D-15-0002.1. URL http://journals.ametsoc.org/doi/10.1175/JHM-D-15-0002.1.